

Final-state interactions in the CP asymmetries of charm-meson two-body decays

Antonio Pich¹, Eleftheria Solomonidi¹, and Luiz Vale Silva¹

*Departament de Física Teòrica, Instituto de Física Corpuscular,
Universitat de València—Consejo Superior de Investigaciones Científicas,
Parc Científic, Catedrático José Beltrán 2, E-46980 Paterna, Valencia, Spain*

 (Received 6 June 2023; accepted 14 July 2023; published 30 August 2023)

Urgent theoretical progress is needed in order to provide an estimate in the Standard Model of the recent measurement by LHCb of direct CP violation in charm-meson two-body decays. Rescattering effects must be taken into account for a meaningful theoretical description of the amplitudes involved in such category of observables, as signaled by the presence of large strong phases. We discuss the computation of the latter effects based on a two-channel coupled dispersion relation, which exploits isospin-zero phase shifts and inelasticity parametrizations of data coming from the rescattering processes $\pi\pi \rightarrow \pi\pi$, $\pi K \rightarrow \pi K$, and $\pi\pi \rightarrow K\bar{K}$. The determination of the subtraction constants of the dispersive integrals relies on the leading contributions to the transition amplitudes from the $1/N_C$ counting, where N_C is the number of QCD colors. Furthermore, we use the measured values of the branching ratios to help in selecting the nonperturbative inputs in the isospin limit, from which we predict values for the CP asymmetries. We find that the predicted level of CP violation is much below the experimental value.

DOI: [10.1103/PhysRevD.108.036026](https://doi.org/10.1103/PhysRevD.108.036026)

I. INTRODUCTION

Symmetries, whether exact or not, played a central role in the formulation of the Standard Model (SM), and offer an avenue to move beyond it. The violation of charge-parity (CP) symmetry in the SM emerges from a single parameter, encoded in the Cabibbo-Kobayashi-Maskawa (CKM) matrix. Whatever the physics that lies beyond the SM (BSM) is, it generally introduces new sources of CP violation, challenging the minimal picture depicted by the SM. Therefore, a prominent way to hunt for BSM physics consists of studying transitions that change quark flavor, and, in particular cases that are sensitive to CP violation. Being a manifestation of the weak sector of the SM, CP -violating observables are sensitive to high energies, helping to collect hints of BSM dynamics beyond the electroweak scale.

The single CP -violating phase of the Kobayashi-Maskawa (KM) mechanism of the SM must be responsible for CP violation across different flavor sectors. This mechanism has been tested in the bottom and strange sectors (see Ref. [1]), but tests in the charm sector are still missing. Other than providing novel tests of the KM mechanism, charm constitutes physics of the up-type

and is then complementary to the down-type sector, which is comparatively better known. In particular, the charm sector offers the opportunity to understand QCD at intermediate energy regimes, namely, in between the light flavors and the bottom, in both of which cases there exist consolidated theoretical tools. Moreover, with charm physics one can also access flavor-changing neutral currents (FCNCs) of the up-type, where a more effective Glashow-Iliopoulos-Maiani (GIM) mechanism applies, which represents an opportunity for clear identification of BSM contributions.

In regard of tests of the KM mechanism, CP violation in the charm sector has been established recently by LHCb [2], which measured the difference of direct CP asymmetries in D^0 decays

$$\Delta A_{CP}^{\text{dir}} = (-15.7 \pm 2.9) \times 10^{-4} \quad (1)$$

between final states involving two charged kaons $A_{CP}(D^0 \rightarrow K^- K^+)$, or two charged pions $A_{CP}(D^0 \rightarrow \pi^- \pi^+)$, where¹

$$\begin{aligned} A_{CP}(i \rightarrow f) &\equiv \frac{|\langle f|T|i\rangle|^2 - |\langle \bar{f}|T|\bar{i}\rangle|^2}{|\langle f|T|i\rangle|^2 + |\langle \bar{f}|T|\bar{i}\rangle|^2} \\ &= \Sigma_j [p_j \sin(\Delta\delta_j) \sin(\Delta\phi_j)]_{i \rightarrow f}, \quad (2) \end{aligned}$$

Published by the American Physical Society under the terms of the Creative Commons Attribution 4.0 International license. Further distribution of this work must maintain attribution to the author(s) and the published article's title, journal citation, and DOI. Funded by SCOAP³.

¹Time integration is left implicit; the contribution of indirect CP violation is negligible [2].

with T being the transition matrix. In order to have a nonvanishing CP asymmetry, one needs both differences of weak ($\Delta\phi$) and strong ($\Delta\delta$) phases, as indicated schematically in the right-hand side of Eq. (2); therein, the sum consists of all possible interference terms j among pairs of amplitudes that have simultaneously different weak [$\Delta\phi_j \neq 0(\text{mod } \pi)$] and strong phases [$\Delta\delta_j \neq 0(\text{mod } \pi)$], and p_j scales like the ratio of a CP -odd over a CP -even amplitude. Weak phases flip sign under the CP transformation, while strong phases are left unchanged. There is an active experimental research program, as attested by the following very recent results [3]:

$$\begin{aligned} A_{CP}(D^0 \rightarrow \pi^- \pi^+) &= (+23.2 \pm 6.1) \times 10^{-4}, \\ A_{CP}(D^0 \rightarrow K^- K^+) &= (+7.7 \pm 5.7) \times 10^{-4} \end{aligned} \quad (3)$$

[which are correlated at the level of 0.88, and the value of $A_{CP}(D^0 \rightarrow \pi^- \pi^+)$ is based on Eq. (1)]. There are also available bounds on CP violation for many other channels (see Appendix A). Much progress is expected in the years to come, thanks to LHCb and Belle II, which will largely improve the sensitivity to sources of CP violation; also, BESIII has an active research program in charm physics. As a benchmark, the accuracy in some CP asymmetries will be improved by about 1 order of magnitude.

On the other hand, theory has to match the observed experimental progress. As previously stated, in the SM the weak phase comes from the CKM matrix. It is yet unknown whether the source of CP violation therein can explain the measurement of $\Delta A_{CP}^{\text{dir}}$, or whether this observable signals the emergence of non-SM sources of CP violation: this is due to the presence of nonperturbative QCD effects that are extremely challenging to describe, precluding precision flavor studies at the present moment. A dynamical mechanism for the generation of the strong phases is the rescattering of on-shell particles, in particular, pion and kaon pairs. It cannot be stressed enough how important the role played by the strong phases in describing CP asymmetries is. Indeed, large strong phases generated in such a dynamical way via rescattering effects are also associated to large modulations of the amplitudes, which must therefore be fully taken into account in predictions of the SM amplitudes. The main interest of this work is the determination of these nonperturbative effects, and their impact on the prediction of the CP asymmetry.

A similar problem happens in the case of kaon decays. The SM description of the measured direct CP violation therein requires the introduction of nonperturbative QCD inputs. Such inputs can be determined via the use of dispersion relations (DRs) [4,5]. The analysis is simpler compared to charm-meson decays, since the only relevant final state accessible from kaon decays are pion pairs, motivating an elastic analysis. In this case, Watson's theorem [6] applies, and the DRs have a known explicit analytical solution [7,8]. Moreover, one also disposes of a

well established effective field theory, which is chiral perturbation theory (χ PT) for the three lightest flavors [9–11]. In order to ensure the convergence of the dispersive integrals and to limit the dependence on the high-energy domain, DRs are eventually “subtracted,” and χ PT provides the subtraction constants of DRs. Alternatively, χ PT provides a framework in which rescattering effects can be computed perturbatively. It is then apparent that DRs provide the resummation of infrared chiral logarithms, which are process independent, while subtraction constants encode the process-dependent ultraviolet dynamics. Importantly, both approaches show a good agreement [4,5,12–16].

In the case of charm physics, we will also employ DRs, which result from two basic principles of any quantum field theory: analyticity (due to causality) and unitarity. In the present case, however, the required analysis is nonelastic because the D^0 mass lies well above the threshold for the production of kaon pairs. We have then a set of integral equations related by unitarity. These equations have to be solved numerically, as no explicit analytical form of the solution is known in general. We are going to include in our analysis only pion and kaon pairs, for which we dispose of abundant data, and neglect further channels in this work. Dealing with other channels requires a different set of techniques, that we postpone to future work. Having pions and kaons, we need as inputs two phase shifts and one inelasticity, which accounts for the probability of transition between pion and kaon pairs; we use available parametrizations for them [17–20]. As in the elastic case of kaon decays into pion pairs, we also need some physical input for the subtraction constants. We employ large- N_C counting for their determination, based on an expansion in powers of $1/N_C$ with N_C , the number of QCD colors [21–23], which is known to provide an understanding of many observed features of nonperturbative strong dynamics [24,25]. Preliminary results were communicated in Refs. [26,27].

Phase shifts and inelasticity at the energy M_D have been applied, nondispersively, in, e.g., Refs. [28–30].² Although they recognize the importance of rescattering effects, these approaches do not capture their full picture, which is the aim of employing a dispersive treatment. Previous discussions of DRs in the context of charm-meson decays include Refs. [32–36], which have not addressed CP violation, which is the main focus here. Compared to these

²Note that Ref. [30] writes for isospin zero:

$$\begin{pmatrix} \mathcal{A}_{D^0 \rightarrow \pi\pi} \\ \mathcal{A}_{D^0 \rightarrow KK} \end{pmatrix} = S_S \begin{pmatrix} V_{cd}^* V_{ud} a_{\pi\pi} \\ V_{cs}^* V_{us} a_{KK} \end{pmatrix} \quad (4)$$

with $a_{\pi\pi}, a_{KK}$ real, which seems not to implement the result expected for the strong phase from Watson's theorem in the limit where the rescattering process is elastic. Also note that Ref. [28] writes $A = S_S^{1/2} A^{\text{bare}}$, where $S_S^{1/2}$ encodes the rescattering part, implementing correctly that limit. For a discussion of the latter approach, see Ref. [31].

references, we discuss DRs and the inputs that we employ in detail.

Various other nondispersive analyses have also been made for the description of multiple charm-meson decay modes, such as topological approaches, the use of $SU(3)_F$ or its sub-groups, transitions assisted by intermediate resonances, etc.; see Refs. [37–54].

Also note that calculations based on QCD light-cone sum rules [55,56] indicate that the SM cannot account for the large level of CP asymmetry observed by LHCb. However, light-cone sum rules have not been extensively tested in the charm sector, requiring alternative methods to support such an extraordinary claim.

Let us also mention that, although methods to deal with rescattering in the lattice [57] are progressing fast, the typical energy scale of charm processes still represents an overwhelming problem for lattice QCD methods.

Having stressed the need for dealing with strong interactions, let us point out that there are ways, however, of extracting properties of weak interactions without the need to describe in detail the strong dynamics. In the charm sector, we are not at that stage yet: we cannot rely on a strategy such as, for instance, the one employed in the extraction of the unitarity angle α from charmless B -meson (quasi-)two-body decays having pions and rhos in the final state, since we do not dispose of the necessary number of measurements at the required level of accuracy to use an isospin analysis [58].

Conversely, the problem we deal with here is less a question of precision as it is in the case of bottom physics, for instance. In that sector, one will face in the (near) future the need for better describing subleading effects (e.g., long-distance penguin effects in the extraction of β , better controlling experimental systematics from decays of charm-mesons in the extraction of γ , dealing with isospin breaking in the extraction of α , etc.). Rather, in the charm sector we cannot rely on the experimental (such as isospin analysis) and theoretical (such as heavy quark expansion, due to the slower convergence of the perturbative series) approaches already employed in the other flavor sectors. It is our goal to employ a data-driven formalism, embodied by the use of DRs.

To conclude this Introduction, note that the large level of CP violation observed in $\Delta A_{CP}^{\text{dir}}$ has triggered studies of contributions from BSM; see Refs. [56,59,60] for recent studies.

This article is organized as follows: in Sec. II we set the relevant weak interactions; in Sec. III we introduce the DRs; their necessary inputs are discussed in Sec. III A, and the numerical solutions of the DRs are given in Sec. III B, while the subtraction constants of once-subtracted DRs are discussed in Sec. III C; in Sec. IV we discuss the available mechanisms of CP violation, and give the predictions for the CP asymmetries; conclusions follow in Sec. V. A series of appendices discuss more technical aspects, and fix possible conventions.

II. EFFECTIVE WEAK INTERACTIONS

The full Hamiltonian at low energies contains (renormalizable) strong and electromagnetic interactions, the kinematic terms for the light quarks and the charm quark (including their masses), and (nonrenormalizable) effective weak interactions. The effective interaction Hamiltonian density for $\Delta C = 1$ up to operators of dimension six, valid for energy scales $\mu_b > \mu > \mu_c$ (μ_q being the energy scale at which the quark of flavor q is integrated out), is the following [61]³:

$$\mathcal{H}_{\text{eff}} = \frac{G_F}{\sqrt{2}} \left[\sum_{i=1}^2 C_i(\mu) (\lambda_d Q_i^d + \lambda_s Q_i^s) - \lambda_b \left(\sum_{i=3}^6 C_i(\mu) Q_i + C_{8g}(\mu) Q_{8g} \right) \right] + \text{H.c.}, \quad (5)$$

where

$$\lambda_q = V_{cq}^* V_{uq}, \quad q = d, s, b. \quad (6)$$

Unitarity of the 3×3 CKM matrix V implies

$$\lambda_d + \lambda_s + \lambda_b = 0. \quad (7)$$

The basis of operators is the following:

$$\begin{aligned} Q_1^d &= (\bar{d}c)_{V-A} (\bar{u}d)_{V-A}, \\ Q_2^d &= (\bar{d}_j c_i)_{V-A} (\bar{u}_i d_j)_{V-A} \stackrel{\text{Fierz}}{=} (\bar{u}c)_{V-A} (\bar{d}d)_{V-A}, \\ Q_1^s &= (\bar{s}c)_{V-A} (\bar{u}s)_{V-A}, \\ Q_2^s &= (\bar{s}_j c_i)_{V-A} (\bar{u}_i s_j)_{V-A} \stackrel{\text{Fierz}}{=} (\bar{u}c)_{V-A} (\bar{s}s)_{V-A}, \\ Q_3 &= (\bar{u}c)_{V-A} \sum_q (\bar{q}q)_{V-A}, \\ Q_4 &= (\bar{u}_j c_i)_{V-A} \sum_q (\bar{q}_i q_j)_{V-A} \\ &\stackrel{\text{Fierz}}{=} \sum_q (\bar{q}c)_{V-A} (\bar{u}q)_{V-A}, \\ Q_5 &= (\bar{u}c)_{V-A} \sum_q (\bar{q}q)_{V+A}, \\ Q_6 &= (\bar{u}_j c_i)_{V-A} \sum_q (\bar{q}_i q_j)_{V+A} \\ &\stackrel{\text{Fierz}}{=} -2 \sum_q (\bar{q}c)_{S-P} (\bar{u}q)_{S+P}, \\ Q_{8g} &= -\frac{g_s}{8\pi^2} m_c \bar{u} \sigma_{\mu\nu} (\mathbf{1} + \gamma_5) G^{\mu\nu} c, \end{aligned} \quad (8)$$

³Indices 1 and 2 are exchanged with respect to Ref. [61], and $C_{1,2}$ ($C_{3,\dots,6}$) are called $z_{2,1}$ (respectively, $v_{3,\dots,6}$) therein. We are not including in the effective Hamiltonian of Eq. (5) either electroweak penguins or the electromagnetic dipole.

where $(V \pm A)_\mu = \gamma_\mu(\mathbf{1} \pm \gamma_5)$, $S \pm P = \mathbf{1} \pm \gamma_5$, and i, j are color indices. The SM Wilson coefficients are fully known to next-to-leading order (NLO) in perturbative QCD, with some next-to-next-to-leading order ingredients available [62]. Their values are given in Appendix A.⁴ Because of the GIM mechanism, (short-distance) penguin operators are absent at scales $\mu > \mu_b$, and result from the NLO matching at μ_b , and the running from μ_b to μ_c ; they come with small Wilson coefficients and thus give suppressed contributions to CP violation. When rescattering effects are large, the main contribution to the CP asymmetries is expected to come from the nonunitarity of the 2×2 CKM submatrix; see Sec. IV A below. This should be contrasted to the case of bottom physics, where rescattering effects are comparatively much smaller, possibly allowing for perturbative treatments.

III. DISPERSION RELATIONS

In describing $D \rightarrow \pi\pi, K\bar{K}$ to first order in weak interactions, a discontinuity equation can be written for the transition amplitudes analytically extended to the complex plane (of the invariant mass squared s of the pseudoscalar pair). The discontinuity is set by the rescattering of the light particles that are stable under strong interactions, with the right-hand cut starting at the threshold for the production of pion pairs, and no left-hand cut for the transition amplitudes; for an introduction, see Ref. [63]. The strong dynamics is nonperturbative in nature and has some useful properties: it conserves flavor, C , P , CP , isospin, and G parity. The rescattering among light, stable final states gives origin to the strong phases necessary for a nonvanishing CP asymmetry. In the elastic limit, such a phase in the weak decay can be extracted directly from the phase shift in the rescattering of pions. More can be learned about the rescattering by exploiting its analyticity in the relevant kinematical variables, relating the dispersive/real and absorptive/imaginary parts of the rescattering amplitudes.

In the little Hilbert space (once the global energy-momentum conservation condition has been factored out), the total S matrix can be written as $S = \mathbf{1} + iT$, which implies the unitarity relation $T - T^\dagger = iTT^\dagger = iT^\dagger T$. In our particular case, S and T are 3×3 matrices describing all possible transitions among the basis of initial and final states $\{D, \pi\pi, K\bar{K}\}$. Restricting to the $\{\pi\pi, K\bar{K}\}$ subspace, the partial-wave (and isospin) projected strong S_S matrix can be written in the form:

$$(S_S)_J^I = (\mathbf{1} + iT_S)_J^I = \mathbf{1} + 2i\Sigma^{1/2}(s)T_J^I(s)\Sigma^{1/2}(s). \quad (9)$$

⁴We indicate Fierz rearrangements when introducing the basis of operators for later convenience; the Wilson coefficients are calculated at the NLO in the un-Fierzed basis. The gluonic dipole does not affect the Wilson coefficients of the penguin operators at NLO in perturbative QCD.

S_S satisfies the unitarity relation $S_S^\dagger S_S = S_S S_S^\dagger = \mathbf{1}$, and T_S inherits $T_S - T_S^\dagger = iT_S T_S^\dagger = iT_S^\dagger T_S$. Since the decaying D mesons are spinless, the total angular momentum of the daughter pair of pseudoscalars is $J = 0$. Owing to Bose symmetry, the two-pion state can have isospin $I = 0$ and 2; the isospin of the kaon pair can take the values $I = 0, 1$. Thus, there are two different isosinglet states that get coupled through the rescattering dynamics. The kinematic factors $\Sigma_i(s) = \Theta(s - 4M_i^2)\sigma_i(s)$ incorporate the threshold conditions and the mass corrections to the two-body center-of-mass three-momenta. In the two-channel isosinglet ($I = 0$) case, $\Sigma(s)$ becomes a 2×2 matrix:

$$\begin{aligned} \Sigma(s) &= \text{diag}[\Theta(s - 4M_\pi^2)\sigma_\pi(s), \Theta(s - 4M_K^2)\sigma_K(s)], \\ \sigma_i(s) &= (1 - 4M_i^2/s)^{1/2}. \end{aligned} \quad (10)$$

The different isospin components of the full amplitudes are given by $T_{\pi\pi}^I(s) \equiv T_{D \rightarrow \pi\pi}^I(s)$ and $T_{KK}^I(s) \equiv T_{D \rightarrow KK}^I(s)$. At lowest order in weak interactions, the unitarity of the S and S_S matrices implies

$$\Sigma^{1/2} \begin{pmatrix} T_{\pi\pi}^0(s + i\epsilon) \\ T_{KK}^0(s + i\epsilon) \end{pmatrix} = (S_S)_0^0 \Sigma^{1/2} \begin{pmatrix} T_{\pi\pi}^0(s - i\epsilon) \\ T_{KK}^0(s - i\epsilon) \end{pmatrix}. \quad (11)$$

We can decompose the full amplitudes as

$$\begin{pmatrix} T_{\pi\pi}^0(s) \\ T_{KK}^0(s) \end{pmatrix} = \Omega^{(0)}(s) \begin{pmatrix} T_{\pi\pi}^{0(B)} \\ T_{KK}^{0(B)} \end{pmatrix}, \quad (12)$$

with the corresponding changes for $I = 1, 2$, where $T_{\pi\pi}^{I(B)}$ and $T_{KK}^{I(B)}$ will be referred to as ‘‘bare amplitudes’’ (for which we will omit their possible s dependence); they are polynomials in s and may contain real zeros, while $\Omega^{(I)}(s)$ has no zeros or poles. As we will see, the bare amplitudes contain the CP -odd phases necessary to generate the CP asymmetries. The rescattering part $\Omega^{(I)}(s)$ of the transition amplitude satisfies then the following discontinuity equation:

$$\begin{aligned} \Omega^{(I)}(s + i\epsilon) &= [\mathbf{1} + 2iT_0^I(s)\Sigma(s)]\Omega^{(I)}(s - i\epsilon) \\ &\equiv S^I(s)\Omega^{(I)}(s - i\epsilon), \end{aligned} \quad (13)$$

where $S^I(s) = \mathbf{1} + 2iT_0^I(s)\Sigma(s)$, with $S^I(s)S^I(s)^* = S^I(s)^*S^I(s) = \mathbf{1}$. This implies

$$\text{Im}\Omega^{(I)}(s + i\epsilon) = T_0^{I*}(s)\Sigma(s)\Omega^{(I)}(s + i\epsilon), \quad (14)$$

after using that $\Omega^{(I)}(s - i\epsilon)^* = \Omega^{(I)}(s + i\epsilon)$ (Schwarz reflection principle). In the following, we will drop ‘‘ $+i\epsilon$ ’’ from $\Omega^{(I)}(s + i\epsilon)$. The analyticity properties of $\Omega^{(I)}(s)$ guarantee that it satisfies the Cauchy integral relation:

$$\Omega^{(I)}(s) = \frac{1}{\pi} \int_{4M_\pi^2}^{\infty} \frac{T_0^{I*}(s') \Sigma(s') \Omega^{(I)}(s')}{s' - s - i\epsilon} ds'; \quad (15)$$

we will later adopt the normalization $\Omega^{(I)}(s_0) = \mathbf{1}$, at a subtraction point s_0 . In the two-channel coupled problem ($I = 0$), we have

$$T_0^0(s) = \begin{pmatrix} \frac{\eta_0^0(s) e^{2i\delta_0^0(s)} - 1}{2i\sigma_\pi(s)} & |g_0^0(s)| e^{i\psi_0^0(s)} \\ |g_0^0(s)| e^{i\psi_0^0(s)} & \frac{\eta_0^0(s) e^{2i(\psi_0^0(s) - \delta_0^0(s))} - 1}{2i\sigma_K(s)} \end{pmatrix}, \quad (16)$$

with the inelasticity parameter

$$\eta_0^0(s) = [1 - 4\sigma_\pi(s)\sigma_K(s)|g_0^0(s)|^2 \times \Theta(s - 4M_\pi^2)\Theta(s - 4M_K^2)]^{1/2}. \quad (17)$$

The sign of the off-diagonal elements of $T_0^0(s)$ is fixed at low energies by χ PT [64], given a choice of convention for the kaon pair isospin decomposition.

One can use that (Sokhotski-Plemelj relation):

$$\frac{1}{x - x_0 - i\epsilon} = P \frac{1}{x - x_0} + i\pi\delta(x - x_0) \quad (18)$$

to write alternatively:

$$\begin{aligned} \text{Re}[\Omega^{(I)}(s)] &= \frac{1}{\pi} \int_{4M_\pi^2}^{\infty} \frac{T_0^{I*}(s') \Sigma(s') \Omega^{(I)}(s')}{s' - s} ds' \\ &= \frac{1}{\pi} \left(\int_{4M_\pi^2}^{4M_K^2} + \int_{4M_K^2}^{\infty} \right) \frac{\text{Im}[\Omega^{(I)}(s')]}{s' - s} ds' \end{aligned} \quad (19)$$

(the slashed integral represents its principal value). Exploiting that the right-hand side is real, we get for the integration domain $s' \geq 4M_K^2$ and any $m \in \{\pi, K\}$:

$$\begin{aligned} &\begin{pmatrix} \text{Re}[(T_0^0)_{\pi\pi}] \sigma_\pi & \text{Re}[(T_0^0)_{\pi K}] \sigma_K \\ \text{Re}[(T_0^0)_{K\pi}] \sigma_\pi & \text{Re}[(T_0^0)_{KK}] \sigma_K \end{pmatrix} \begin{pmatrix} \text{Im}[\Omega_{\pi m}^{(0)}] \\ \text{Im}[\Omega_{K m}^{(0)}] \end{pmatrix} \\ &= \begin{pmatrix} \text{Im}[(T_0^0)_{\pi\pi}] \sigma_\pi & \text{Im}[(T_0^0)_{\pi K}] \sigma_K \\ \text{Im}[(T_0^0)_{K\pi}] \sigma_\pi & \text{Im}[(T_0^0)_{KK}] \sigma_K \end{pmatrix} \begin{pmatrix} \text{Re}[\Omega_{\pi m}^{(0)}] \\ \text{Re}[\Omega_{K m}^{(0)}] \end{pmatrix}. \end{aligned} \quad (20)$$

Admitting that the 2×2 matrix on the left-hand side is invertible (the matrix $T_0^0 \Sigma$ is invertible), then one can solve for $\text{Im}[\Omega^{(0)}] \equiv b$, which is plugged into the previous integral equation for the integration range $s' \geq 4M_K^2$: indeed, this matrix equation can be written as $\mathbf{R} \cdot b_m = \mathbf{I} \cdot a_m \Leftrightarrow b_m = \mathbf{R}^{-1} \cdot \mathbf{I} \cdot a_m$ if \mathbf{R} invertible, with obvious correspondence with Eq. (20). In the integration interval $4M_\pi^2 \leq s' \leq 4M_K^2$ we have, like in the uncoupled case (and consider $\psi_0^I = \delta_0^I \bmod \pi$ in this region),

$$\text{Re}[(T_0^I)_{j\pi}] \text{Im}[\Omega_{\pi m}^{(I)}] = \text{Im}[(T_0^I)_{j\pi}] \text{Re}[\Omega_{\pi m}^{(I)}]. \quad (21)$$

The adopted strategy is to solve for the real parts, and then use the previous relations to determine the imaginary parts. Then

$$\begin{aligned} a_m &= \frac{1}{\pi} \int_{4M_\pi^2}^{4M_K^2} ds' \frac{1}{s' - s} \\ &\times \begin{pmatrix} \tan \delta_0^0(s') & 0 \\ |g_0^0(s')| \sigma_\pi(s') / \cos(\delta_0^0(s')) & 0 \end{pmatrix} \cdot a_m \\ &+ \frac{1}{\pi} \int_{4M_K^2}^{\infty} ds' \frac{\mathbf{R}^{-1} \cdot \mathbf{I} \cdot a_m}{s' - s}. \end{aligned} \quad (22)$$

We then solve for both a_π and a_K , and the final solution is

$$\text{Re}[\Omega^{(0)}] = (a_\pi \otimes a_K), \quad \text{Im}[\Omega^{(0)}] = (b_\pi \otimes b_K), \quad (23)$$

where \otimes means that we combine the two dimension-two vectors represented as columns into a 2×2 matrix. Note that $\Omega^{(0)}(s_0) = \mathbf{1}$ implies that a_π and a_K are independent, and a similar comment applies for the imaginary parts b_π and b_K . The system of independent functions $\chi^{(k)}(s) \equiv a_k + ib_k$ built from these real and imaginary parts is called a *fundamental system of solutions* satisfying the discontinuity problem of Eq. (13); see Ref. [7]. There are n such solutions in an n -channel coupled case. A similar discussion holds for once-subtracted DRs. The use of subtracted DRs limits the dependence to high-energy data, which are typically less accurate or even missing; they may also be necessary in order to guarantee the convergence of the dispersive integrals.

In the elastic limit, one can solve the integral equation explicitly [7,8]. Considering one subtraction:

$$\Omega^{(I)}(s) = \exp\{i\delta_0^I(s)\} \exp\left\{\frac{s - s_0}{\pi} \int_{4M_\pi^2}^{\infty} \frac{dz}{z - s_0} \frac{\delta_0^I(z)}{z - s}\right\}, \quad (24)$$

where $s_0 \leq 4M_\pi^2$ is the subtraction point, at which we have imposed $\Omega^{(I)}(s_0) = 1$. The rightmost exponential above carries no zeros nor poles for well-behaved phase shifts; it is obviously non-negative. It is manifest that large phase shifts are associated to large modulations of $|\Omega^{(I)}(s)|$. The phase shift and the Omnès factor $|\Omega^{(I)}(s)|$ encode the effects of rescattering, and are necessary for a good qualitative and quantitative description of the transition amplitudes in the weak decay. It is important to stress the universal character of this equation, which depends only on the phase shift, and not the particular electroweak process under discussion.

The previous equation leads to the following asymptotic behavior (see e.g. Ref. [63]):

$$\Omega^{(l)}(s) \rightarrow s^x, \quad x = -\frac{\delta_J^l(\infty) - \delta_J^l(4M_\pi^2)}{\pi}, \quad (25)$$

where at threshold $\delta_J^l(4M_\pi^2) = 0$. Therefore, if the Omnès factor is supposed to vanish asymptotically, as it is expected when building form factors from the latter rescattering factor (see e.g. Ref. [65]), in the single-channel analysis one requires $\delta_J^l(\infty) > \delta_J^l(4M_\pi^2)$.

In the inelastic case, the determinant of $\Omega^{(l)}(s)$ has an explicit analytical solution, from which a similar discussion holds. In the two-channel analysis, for instance, Eq. (13) leads to

$$\det \Omega^{(l)}(s + i\epsilon) = \exp \{2i\psi_J^l(s)\} \det \Omega^{(l)}(s - i\epsilon), \quad (26)$$

which does not depend on the inelasticity.⁵ A property of the fundamental system of solutions is that the individual indices x_k , describing the asymptotic behaviour of the fundamental solutions $\chi^{(k)}(s)$, do not depend on the particular choice of the fundamental system of solutions (see also next paragraph). Their sum satisfies the relation [7]:

$$\sum_{k=1}^n x_k = x, \quad (27)$$

where x is the index resulting from taking the determinant of Eq. (13) in the n -channel coupled analysis. For instance, in the two-channel problem under discussion, $x = -(\psi_0^0(\infty) - \psi_0^0(4M_\pi^2))/\pi$.

Regarding the asymptotic behavior, we comment on a specific case of later interest: if the sum of indices is $x = -2$, then one can have two independent solutions that vanish asymptotically and simultaneously, i.e., both having indices $x_1 = -1$ and $x_2 = -1$. If on the other hand the sum of indices is $x = -3$, for instance, then one can have two solutions that vanish asymptotically, i.e., $x_i = -2$ and -1 , but they are not unique: to the solution that goes as -1 one can add a contribution from the one that goes as -2 (times a polynomial of degree up to 1) and take this as the fundamental solution that replaces the previous one, while keeping the condition $\Omega^{(l)}(s_0)$ at a subtraction point s_0 . In such cases, more physical information about the sought solutions has to be provided [66].

A. Experimental inputs for the DRs

Hereafter we discuss datasets and parametrizations of the inputs for DRs in isospin zero and isospin two. We point out the main qualitative features observed in phase shifts and inelasticity, shown in Figs. 1–3. We take

⁵We note that we have not been able to find a function of the two-channel Omnès matrix other than its determinant that does not depend on the inelasticity, for which there is an explicit analytical solution.

the constrained fits to data enforcing dispersive relations of Refs. [17–20], which we discuss in more detail below.

1. Isospin-zero phase shift of pion pairs

We use the analyses of Refs. [18,19]. As seen from the top-left panel of Fig. 1, the phase shift starts at zero at the pion pair production threshold, and shows a steady increase sufficiently below the threshold for kaon pair production, due to the presence of the σ resonance, which is located deep into the first Riemann sheet, away from the real axis. Then, there is a quick increase of the phase shift, due to the presence of the $f_0(980)$ resonance, which is relatively narrow. Another analytical feature in the region ~ 1 GeV is the threshold for kaon pair production. Subsequently, the phase shift grows steadily; in this energy region there exist the well-established resonances $f_0(1370)$, $f_0(1500)$, and $f_0(1710)$, which to some extent overlap among themselves [for a recent discussion of $f_0(1370)$, see Ref. [67]].

Above around 1.42 GeV, Ref. [19] considers different datasets, which are not consistent among themselves, providing purely descriptive phase-shift parametrizations separately for each of them; see the top-right panel of Fig. 1. Solution I [68–71] follows from a dataset that extends up to $E_0 = 1.9$ GeV, while the datasets leading to solutions II [72] and III [73] extend up to $E_0 = 1.8$ GeV.

2. Isospin-zero phase shift of kaon pairs

We consider the combined analysis of $\pi\pi \rightarrow KK$ and $K\pi \rightarrow K\pi$ employing crossing symmetry of Ref. [20]; see also Ref. [74]. There are two possible solutions, B and C, that are well compatible; see the bottom-left panel of Fig. 1 (see also comments below). The curve extends up to $E_0 = 2$ GeV. There is a clear structure in the phase shift in the region 1.2–2 GeV, that might be in part due to the isoscalar-scalar resonances mentioned above, with the phase shift decreasing at times.⁶

3. Isospin-zero inelasticity

Below the threshold for their on-shell production, virtual kaon pairs produce off-diagonal elements in the two-channel rescattering matrix, with their impact seen in the first term in the right-hand side of Eq. (22). They do not produce an absorptive part though; i.e., they do not alter the evolution of the phase motion, and the off-diagonal phase shift therein is then the one observed in pion pair rescattering. Note, however, that it does not mean that the inelasticity below the kaon pair threshold varies, being

⁶There is an interesting result in quantum mechanics, according to which the phase shift cannot decrease too quickly in order to respect causality; see Ref. [75] and, e.g., Refs. [76,77]. In the present situation, we observe that $-2\hbar c \frac{d\psi_0^0(E^2)}{dE} \lesssim 4$ fm, which gives a crude estimate of the minimum range of the potential as required from causality.

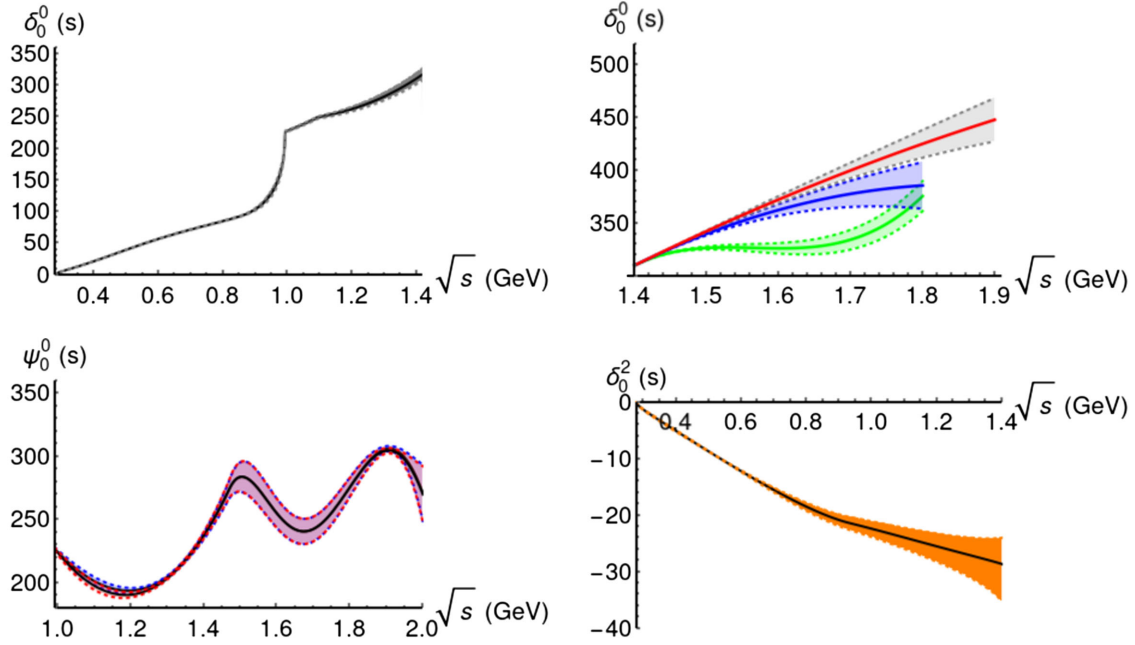


FIG. 1. Set of phase shifts from Refs. [17–20] used in our analysis. The $\delta_0^0(s)$ phase is shown in the upper panels for $2M_\pi \leq \sqrt{s} \leq 1.42$ GeV (top, left) and $\sqrt{s} \geq 1.4$ GeV (top, right), where solutions I (gray), II (blue), and III (green) are given. The $\psi_0^0(s)$ phase is shown in the (bottom, left), for solutions B (blue) and C (red), which are very compatible; below the kaon pair threshold, $\psi_0^0(s) = \delta_0^0(s)$. The $\delta_0^2(s)$ phase is shown in the (bottom, right), up to $\sqrt{s} = 1.4$ GeV and starting from the pion pair threshold. All phases are given in degrees.

$\eta_0^0 = 1$ below this threshold. We consider Refs. [20,78] for a parametrization of such effect, illustrated in the left panel of Fig. 2 (for definiteness, when not specified we employ solution B below), see also Ref. [74].

The inelasticity η_0^0 can be extracted from the off-diagonal T -matrix element $|g_0^0|$ via a combined analysis of $\pi\pi \rightarrow KK$ and $K\pi \rightarrow K\pi$, and is available up to $E_0 = 2$ GeV, as illustrated in the right panel of Fig. 2. This leads to two solutions, B [79] and C [80,81], corresponding to inconsistent datasets below ~ 1.47 GeV, and thus their parametrizations of the inelasticity differ substantially below that point. We combine the effect generated by off-shell kaon pairs [20,78] with the explicit parametrizations found in Ref. [20] valid above $2M_K$. The two sets of curves are

combined at a matching point of $\sqrt{1.2}$ GeV [78], and the corresponding solutions will be called B' and C' in the following. There is a very small discontinuity at the matching scale (of 9% for solution B' and of 8% for solution C'). Right above the kaon pair threshold and below the matching scale, there is a short window in which the unitarity bound is violated, manifested as the impossibility of defining a real inelasticity therein via the use of Eq. (17). However, this corresponds to a tiny region (long of ~ 30 MeV for solution B' and of ~ 10 MeV for solution C'), in which we set the inelasticity to zero.

An alternative for the extraction of the inelasticity η_0^0 is to look directly at the rescattering process $\pi\pi \rightarrow \pi\pi$. The extraction of the parametrization for the phase shift of the

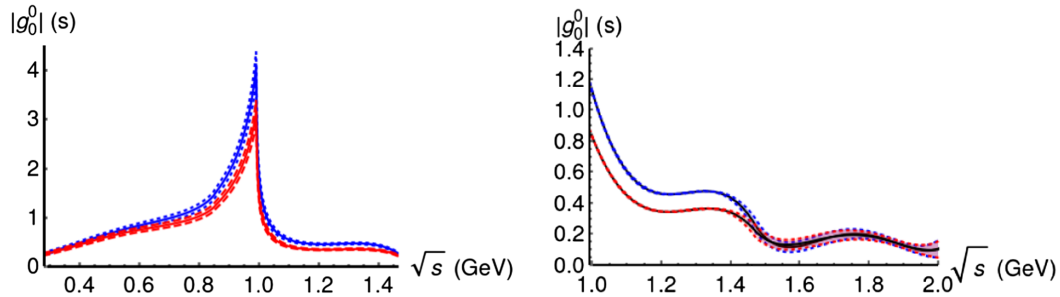


FIG. 2. Off-diagonal T -matrix element from Ref. [20] for solutions B (blue) and C (red). The two sets, valid along the energy ranges from the pion pair threshold and up to 1.47 GeV (left) and from the kaon pair threshold and up to 2 GeV (right), are combined according to the procedure described in the text.

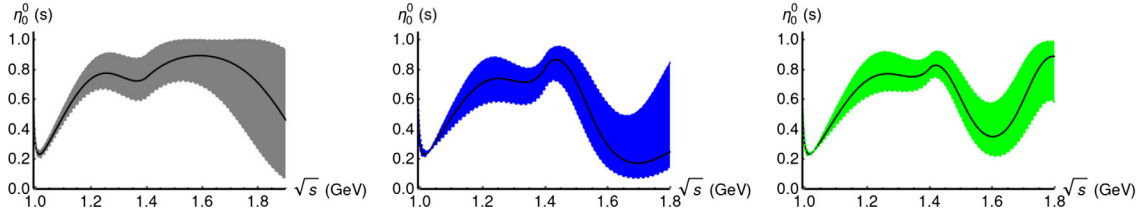


FIG. 3. Inelasticity from Ref. [19] extracted from pion pair rescattering. Below the kaon pair threshold, $\eta_0^0(s) = 1$. Three solutions are shown, namely, solutions I (left), II (center) and III (right).

pion pair system discussed above is done simultaneously to the extraction of the parametrization for the inelasticity, for which then we also have three solutions [19], illustrated in Fig. 3. As before, solution I extends up to $E_0 = 1.9$ GeV, while solutions II and III extend up to $E_0 = 1.8$ GeV. (We correct typos found in Ref. [19], namely, ϵ_4 in their Table 2 comes with the wrong sign, and K_i must be multiplied by M_K^2 [78].) Solution III shows a sharp dip in the inelasticity around ~ 1.6 GeV, and a distinguishing phase motion compared to the other two solutions, which may signal the presence of the resonance $f_0(1500)$. As further discussed later, inelasticities extracted in this way carry large uncertainties. At the energy $2M_K$, the off-diagonal element resulting from this inelasticity is combined with the one from Refs. [20,78], which describes off-shell kaon pairs. This produces an abrupt change across a few MeV of the off-diagonal T -matrix element at about $2M_K$, which is expected to have a limited impact on the fundamental Omnès solutions far away from this value of the energy. Moreover, combining the two curves at $2M_K$ generates a consistent trend, since below (above) $2M_K$ the modulus of the off-diagonal T -matrix is decreasing (increasing) quickly with increasing (decreasing) energies.

The different sets of inelasticities discussed above, solutions I–III and solutions B' and C', display important differences. In discussing solutions of the dispersive equations, we will show results for each of them separately.

4. Isospin-two phase shift and inelasticity of pion pairs

The phase shift starts at zero at the pion pair production threshold, and decreases steadily in the region extending up to about 1.45 GeV [82–84]. A parametrization is provided by Refs. [17,85]; see the bottom-right panel of Fig. 1, which does not include Ref. [86]. The extracted inelasticity is close to the elastic limit in that energy range [17].

Although to our knowledge a parametrization is not available (in particular, taking into account dispersive constraints), Ref. [86] extracts data up to 2.2 GeV. It is seen that the phase shift has the tendency to decrease up to 1.3 GeV, and then to increase subsequently. At around M_D , the phase shift equals a few negative degrees, but carries a large uncertainty. There seems to be a large inelasticity at around M_D , although again large uncertainties are present. [This overall behavior of the phase shift can be reproduced

via an elastic analysis relying on χ PT and resonance chiral theory ($R\chi$ T), with a t -channel exchange of ρ , etc.; see also Ref. [87].]

As discussed above around Eq. (25), the phase shift in an elastic analysis should become positive (vanish) so that the Omnès solution goes to zero (respectively, a constant) at infinity. This requires some underlying physics to change the sign of the isospin-two phase shift, such as the presence of a resonance. We also note that no distinct feature is seen in the isospin-two $\pi\pi \rightarrow \pi\pi$ study of Ref. [88], for which however contributions to the cross section other than the S wave become increasingly important at higher energies.

We will later in the text extract the Omnès factor $|\Omega^{(2)}|$ from the branching ratio of the charged decay mode $D^+ \rightarrow \pi^0\pi^+$, and vary the isospin-two phase shift to reproduce the $D^0 \rightarrow \pi^-\pi^+, \pi^0\pi^0$ branching ratios. We reserve further discussion about the isospin-two inelasticity to future work [89].

B. Solutions of the coupled channel DRs

To employ the DRs, we extrapolate the phase shift and inelasticity curves discussed above beyond their indicated endpoints $E_0 = 1.8$ – 2 GeV [90]:

$$\begin{aligned} \delta_0^0(E) &= n^*\pi + (\delta_0^0(E_0) - n^*\pi)f_\delta\left(\frac{E}{E_0}\right), \\ \delta_K(E) &= \ell^*\pi + (\delta_K(E_0) - \ell^*\pi)f_\delta\left(\frac{E}{E_0}\right), \end{aligned} \quad (28)$$

where the chosen $f_\delta(x) = 2/(1+x^{m_\delta^*})$ has the virtue of being a smooth function connecting the values at the endpoints to the asymptotic values (Ref. [90] takes $m_\delta^* = 3$; we note that the asymptotic behavior of the phase shift involved in the vector form factor of the pion is discussed in Ref. [91]). The values of $n^* + \ell^* \geq 2$ ensure that at least one of the fundamental solutions tends to zero at infinite energies. We take n^*, ℓ^* as integer values (as it results from having resonant effects; i.e., we neglect non-resonant effects for this sake). Then, we set $\ell^* = -1$ since $\delta_K(E) \equiv \psi_0^0(E) - \delta_0^0(E)$ is close to $-\pi$ at E_0 . Finally, we take $n^* = 3$. It suffices to ensure the good behavior of the fundamental solutions, as it leads in practice to two independent solutions of indices $x_{1,2} = -1$. These

TABLE I. Sample of Omnès solutions at $s = M_D^2$. In the main text, the case of solution I for the phase shift and the inelasticity $\eta_0^0 - \delta\eta_0^0$, with $m_\eta^* = 2$, is referred to as the reference case.

	Solution I	Solution II	Solution III
$\eta_0^0, m_\eta^* = 1$	$\Omega^{(0)} = \begin{pmatrix} 0.80e^{+1.60i} & 1.01e^{-1.69i} \\ 0.56e^{-1.50i} & 0.59e^{+2.07i} \end{pmatrix}$	$\Omega^{(0)} = \begin{pmatrix} 0.39e^{+1.64i} & 0.59e^{-2.13i} \\ 0.51e^{-1.31i} & 0.56e^{+2.43i} \end{pmatrix}$	$\Omega^{(0)} = \begin{pmatrix} 0.71e^{+0.53i} & 1.35e^{-2.67i} \\ 0.38e^{-0.98i} & 0.42e^{+2.65i} \end{pmatrix}$
$\eta_0^0 - \delta\eta_0^0, m_\eta^* = 1$	$\Omega^{(0)} = \begin{pmatrix} 0.56e^{+1.84i} & 0.61e^{-1.73i} \\ 0.57e^{-1.41i} & 0.58e^{+2.25i} \end{pmatrix}$	$\Omega^{(0)} = \begin{pmatrix} 0.42e^{+1.75i} & 0.54e^{-2.05i} \\ 0.51e^{-1.33i} & 0.55e^{+2.43i} \end{pmatrix}$	$\Omega^{(0)} = \begin{pmatrix} 0.35e^{+1.13i} & 0.74e^{-2.47i} \\ 0.50e^{-1.18i} & 0.55e^{+2.48i} \end{pmatrix}$
$\eta_0^0 - \delta\eta_0^0, m_\eta^* = 2$	$\Omega^{(0)} = \begin{pmatrix} 0.58e^{+1.80i} & 0.64e^{-1.74i} \\ 0.58e^{-1.37i} & 0.61e^{+2.26i} \end{pmatrix}$	$\Omega^{(0)} = \begin{pmatrix} 0.43e^{+1.64i} & 0.58e^{-2.10i} \\ 0.52e^{-1.25i} & 0.57e^{+2.48i} \end{pmatrix}$	$\Omega^{(0)} = \begin{pmatrix} 0.40e^{+1.01i} & 0.80e^{-2.50i} \\ 0.50e^{-1.11i} & 0.56e^{+2.53i} \end{pmatrix}$
$\eta_0^0 - \delta\eta_0^0, m_\eta^* = 3$	$\Omega^{(0)} = \begin{pmatrix} 0.60e^{+1.76i} & 0.66e^{-1.74i} \\ 0.60e^{-1.33i} & 0.63e^{+2.26i} \end{pmatrix}$	$\Omega^{(0)} = \begin{pmatrix} 0.44e^{+1.53i} & 0.61e^{-2.16i} \\ 0.52e^{-1.17i} & 0.59e^{+2.53i} \end{pmatrix}$	$\Omega^{(0)} = \begin{pmatrix} 0.45e^{+0.91i} & 0.86e^{-2.53i} \\ 0.50e^{-1.04i} & 0.57e^{+2.58i} \end{pmatrix}$
Solution B': $ g_0^0 $	$\Omega^{(0)} = \begin{pmatrix} 2.01e^{+1.39i} & 2.47e^{-1.76i} \\ 0.37e^{-0.33i} & 0.54e^{+3.05i} \end{pmatrix}$	$\Omega^{(0)} = \begin{pmatrix} 1.91e^{+0.60i} & 2.78e^{-2.55i} \\ 0.31e^{-0.23i} & 0.45e^{+3.30i} \end{pmatrix}$	$\Omega^{(0)} = \begin{pmatrix} 2.20e^{+0.43i} & 3.55e^{-2.72i} \\ 0.35e^{+0.03i} & 0.57e^{+3.40i} \end{pmatrix}$
Solution C': $ g_0^0 $	$\Omega^{(0)} = \begin{pmatrix} 1.83e^{+1.38i} & 2.65e^{-1.76i} \\ 0.34e^{-0.40i} & 0.57e^{+3.00i} \end{pmatrix}$	$\Omega^{(0)} = \begin{pmatrix} 1.80e^{+0.59i} & 3.11e^{-2.56i} \\ 0.29e^{-0.24i} & 0.49e^{+3.24i} \end{pmatrix}$	$\Omega^{(0)} = \begin{pmatrix} 2.09e^{+0.43i} & 3.94e^{-2.72i} \\ 0.32e^{-0.03i} & 0.61e^{+3.34i} \end{pmatrix}$

solutions are uniquely determined, after specifying the condition $\Omega^{(0)}(s_0) = \mathbf{1}$ at the subtraction point s_0 .

A similar extrapolation is taken for the inelasticity:

$$\eta_0^0(E) = \eta_\infty + (\eta_0^0(E_0) - \eta_\infty) f_\eta \left(\frac{E}{E_0} \right). \quad (29)$$

Its limiting value is set to $\eta_\infty = 1$. Together with the limit values of the phase shifts, these conditions satisfy the asymptotic behavior discussed in Ref. [92]. Large values of m_η^* (i.e., η_0^0 approaching faster its asymptotic value) would require some underlying dynamics, such as the appearance of resonances not yet firmly established [93], and for this reason we later display only values in the range $m_\eta^* \in \{1, 2, 3\}$.

To full generality, there is no known explicit solution in the inelastic case. The numerical method used is described in Appendix B (we discuss an explicit solution valid under certain conditions in Appendix C), and relies on the parametrization of data previously discussed.⁷

A sample of typical Omnès matrices is provided in Table I for various scenarios: columns correspond to solutions I–III for the phase- shifts, and also inelasticity; the first block of rows corresponds to the inelasticity directly extracted from $\pi\pi \rightarrow \pi\pi$, while the second block of rows corresponds to the inelasticity calculated from the off-diagonal T -matrix element as in Eq. (17), for which there are solutions B' and C'. We observe a strong dependence of the Omnès solution with the inelasticity employed, which in the case of the first block of rows

carries a large uncertainty. Varying the latter uncertainties leads to profiles $\eta_0^0 - \delta\eta_0^0$, which seek to saturate the error bars attached to the inelasticities found in Ref. [19] towards smaller values of η_0^0 .⁸ In a companion paper, we provide a discussion of CP asymmetries that does not depend on the input employed for the inelasticity [96].

When calculating the Omnès matrices, we verify that $\Omega_{11}^{(0)}(M_K^2)$ is in good agreement with a similar calculation relying on an elastic analysis [4,5]: were there a sizable difference, it would spoil the good comparison with the χ PT calculation of this same quantity.

C. Partial-wave transition amplitudes

In order to build transition amplitudes from the rescattering effects encoded in $\Omega^{(0)}(s)$ (or analogously for isospin one and two, which we treat elastically), we need to specify the polynomial ambiguities in $T_{\pi\pi}^{0(B)}$ and $T_{KK}^{0(B)}$ of the once-subtracted DRs. Summing over the possible solutions to the two-channel coupled analysis problem, times subtraction constants, we have

$$\begin{pmatrix} T_{\pi\pi}^0(s) \\ T_{KK}^0(s) \end{pmatrix} = \begin{pmatrix} \Omega_{11}^{(0)}(s) & \Omega_{12}^{(0)}(s) \\ \Omega_{21}^{(0)}(s) & \Omega_{22}^{(0)}(s) \end{pmatrix} \begin{pmatrix} T_{\pi\pi}^{0(B)} \\ T_{KK}^{0(B)} \end{pmatrix}, \quad (30)$$

where since we deal with charmed-meson decays, $s \rightarrow M_D^2$.

The polynomials $T_{\pi\pi}^{0(B)}$ and $T_{KK}^{0(B)}$ are fixed by physical considerations relying on a large- N_C expansion. In the limit $N_C \rightarrow \infty$, the scattering phase shifts are exactly zero and, therefore, $\Omega^{(l)}(s) = \mathbf{1}$. Moreover, in this limit the hadronic

⁷In the N/D method, phase-shift parametrizations and Omnès functions are extracted simultaneously in the fits to the rescattering data [94,95].

⁸Possible correlations among the different uncertainties for phase shifts and inelasticity are neglected here.

matrix elements of the short-distance four-quark operators factorize into matrix elements of QCD currents. The bare amplitudes $T_{\pi\pi}^{0(B)}$ and $T_{KK}^{0(B)}$ correspond then to tree insertions of different local operators, current-current and penguin ones, while topologies beyond trees are generated via rescattering effects. The factorized expressions are written in terms of decay constants and form factors (e.g., $D \rightarrow \pi$, or $D \rightarrow K$), given in Appendices D and E. It follows from the present discussion that the subtraction constants require perturbative and nonperturbative elements: decay constants, form factors, and Wilson coefficients. As it has been discussed, rescattering is taken into account dispersively, and it is in fact suppressed in the large- N_C counting. Decay constants and form factors also integrate nonperturbative QCD effects that, although sub-leading in the large- N_C counting, are not included in the rescattering matrix $\Omega^{(I)}(s)$. Note that the resulting subtraction constants are real (in the CP -conserving limit), strong complex phases being developed in the rescattering. In the context of $K \rightarrow \pi\pi$ transitions, the polynomial ambiguities can be determined via χ PT [4,5]. (For a discussion of form factors built from the same rescattering effects, their asymptotic behavior, and the use of χ PT to determine the subtraction constants, see, e.g., Refs. [64,90,97–99].)

The subtraction point is taken at $s_0 = M_\pi^2$, as suggested by $T_{\pi\pi}^{0(B)} \propto M_D^2 - M_\pi^2$. At this point, $\Omega^{(0)}$ is set to the identity $\mathbf{1}$. Any modulation of $\Omega^{(0)}$ above s_0 results then from rescattering effects. We observe, however, a very small dependence with the choice of the subtraction point, as seen from the two following solutions:

$$\begin{aligned} \Omega^{(0)}(M_D^2) &= \begin{pmatrix} 0.59e^{+1.81i} & 0.64e^{-1.74i} \\ 0.59e^{-1.38i} & 0.62e^{+2.26i} \end{pmatrix}, & s_0 = 0, \\ \Omega^{(0)}(M_D^2) &= \begin{pmatrix} 0.57e^{+1.71i} & 0.61e^{-1.72i} \\ 0.56e^{-1.27i} & 0.58e^{+2.24i} \end{pmatrix}, & s_0 = 4M_\pi^2, \end{aligned} \quad (31)$$

which are calculated with the same inputs as used for the so-called reference case of Table I to be discussed below, but with different subtraction points. Moreover, given that $M_\pi^2, M_K^2 \ll M_D^2$, we observe a very small numerical impact of keeping the masses of the light mesons with respect to neglecting them in the expressions of the physical observables.

IV. THEORETICAL PREDICTIONS

Before moving to the numerical predictions for branching ratios and CP asymmetries, we first discuss the mechanisms at play responsible for generating a non-vanishing level of CP violation. Detailed technical discussions are given in a series of appendices: Appendix D

discusses the relevant decay constants and form factors, Appendix E gives the expressions for the bare decay amplitudes, and the isospin decomposition of the transition matrix elements is detailed in Appendix E 1.

A. Mechanisms of CP violation

We consider tree insertions of the short-distance operator basis provided in Eq. (8), whose matrix elements can be found in Appendix E. The CP -violating effects are generated through the interference of amplitudes with different weak and strong phases. Let us consider first the isospin-zero decay amplitudes that exhibit the CKM structure displayed in Eq. (5):

$$\begin{aligned} \begin{pmatrix} T_{\pi\pi}^0(s) \\ T_{KK}^0(s) \end{pmatrix} &= \Omega^{(0)}(s) \begin{pmatrix} \lambda_d T_{\pi\pi}^{CC} - \lambda_b T_{\pi\pi}^P \\ \lambda_s T_{KK}^{CC} - \lambda_b T_{KK}^P \end{pmatrix} \\ &\equiv \begin{pmatrix} \mathcal{A}_0^\pi + i\mathcal{B}_0^\pi \\ \mathcal{A}_0^K + i\mathcal{B}_0^K \end{pmatrix}. \end{aligned} \quad (32)$$

The uncoupled $I = 1$ and 2 amplitudes can also be written in a similar (simpler) way. The CP -even strong phases are generated by the rescattering matrices $\Omega^{(I)}$, while the CP -odd weak phases originate in the CKM factors λ_q appearing in the bare amplitudes, which are different for current-current ($T_{\pi\pi, KK}^{CC}$) and penguin ($T_{\pi\pi, KK}^P$) operators. We have decomposed the full decay amplitudes into their CP -even (\mathcal{A}_I) and CP -odd (\mathcal{B}_I) components. Obviously, the \mathcal{A}_I amplitudes depend on the parameters $\text{Re}\{\lambda_q\}$, while \mathcal{B}_I are governed by $\text{Im}\{\lambda_q\}$. Despite the different sizes of their corresponding Wilson coefficients, $T_{\pi\pi, KK}^{CC} \sim T_{\pi\pi, KK}^P$ due to the large pre-factors coming with Q_6 insertions; see Appendix E.

Observable effects must be stated in terms of rephasing-invariant quantities. Other than the quartets

$$Q_{ai\beta j} \equiv V_{ai} V_{\beta j} V_{\alpha j}^* V_{\beta i}^*, \quad (33)$$

rephasing-invariant objects also include the moduli of the elements of the CKM matrix; for a review, see Ref. [100]. The relevant rephasing-invariant quantities have the following numerical values:

$$\begin{aligned} Q_{udcb} &= -A^2 \lambda^6 (\rho + i\eta) + \mathcal{O}(\lambda^8) \\ &\simeq -(1.3 + i3.1) \times 10^{-5}, \\ Q_{udcs} &= -\lambda^2 + \lambda^4 + A^2 \lambda^6 (1 - \rho + i\eta) + \mathcal{O}(\lambda^8) \\ &\simeq -0.048 + i3.1 \times 10^{-5}, \\ Q_{uscb} &= A^2 \lambda^6 (\rho + i\eta) + \mathcal{O}(\lambda^8) \simeq (1.3 + i3.1) \times 10^{-5}, \end{aligned} \quad (34)$$

and

$$\begin{aligned}
|\lambda_d|^2 &= \lambda^2 + \mathcal{O}(\lambda^4) \simeq 0.051, \\
|\lambda_s|^2 &= \lambda^2 + \mathcal{O}(\lambda^4) \simeq 0.051, \\
|\lambda_b|^2 &= A^4 \lambda^{10} (\rho^2 + \eta^2) + \mathcal{O}(\lambda^{12}) \simeq 2.3 \times 10^{-8}. \quad (35)
\end{aligned}$$

Note that λ_d and λ_s cannot be chosen simultaneously real, since the quartets $Q_{\alpha\beta j}$ are rephasing invariant and $Q_{udcs} = V_{ud}V_{cs}V_{us}^*V_{cd}^* = \lambda_d\lambda_s^*$. This is particularly important in the presence of rescattering effects, under which the isoscalar amplitudes depend on both λ_d and λ_s . (Numerical values of $\text{Re}\{\lambda_q\}$ and $\text{Im}\{\lambda_q\}$, $q = d, s, b$, in the usual convention for the CKM matrix elements are found in Appendix A.)

Thus, the rescattering of the final pseudoscalar mesons generates a pure $I = 0$ contribution to the CP asymmetries, originating in the interference of the intermediate $\pi\pi$ and KK contributions. Written in a rephasing-invariant way, the full contribution of isospin-zero-only amplitudes to the numerator of the direct CP asymmetries is given by

$$\text{num}(A_{CP}^i)_{I=0} = 4\omega_i^{(\text{Im})} J(T_{\pi\pi}^{CC}T_{KK}^{CC} + T_{\pi\pi}^{CC}T_{KK}^P + T_{\pi\pi}^PT_{KK}^{CC}). \quad (36)$$

This contribution is governed by the Jarlskog parameter $J = \text{Im}\{Q_{udcs}\} = r_{\text{CKM}}|\lambda_d|^2$, where $r_{\text{CKM}} \equiv \text{Im}\{\lambda_b/\lambda_d\}$, and the dynamical rescattering factors

$$\omega_i^{(\text{Im})} \equiv \text{Im}\{\Omega_{i1}^{(0)*}\Omega_{i2}^{(0)}\}. \quad (37)$$

The quantity $\omega_\pi^{(\text{Im})} \equiv \omega_1^{(\text{Im})}$ ($\omega_K^{(\text{Im})} \equiv \omega_2^{(\text{Im})}$) controls the amount of CP violation in $D^0 \rightarrow \pi\pi$ (respectively, $D^0 \rightarrow KK$) coming exclusively from the interference of isospin-zero contributions. The possibility of having a source of CP violation coming exclusively from isospin-zero amplitudes has been pointed out by, e.g., Ref. [29]. Such a case is not possible in kaon decays, since the dynamics therein is elastic.

The source of CP violation coming from current-current operators, due to the nonunitarity of the 2×2 CKM submatrix, and the suppression of contributions from penguin operators due to small Wilson coefficients have often been pointed out in the literature; see, e.g., Refs. [55, 101]. Note, however, that in Ref. [43] the quantity analogous to $T_{\pi\pi, KK}^P$ generates the needed CP -odd amplitude, in a mechanism in which the operators $Q_{5,6}$ couple D^0 to $f_0(1710)$, which subsequently decays to pion and kaon pairs. The state $f_0(1710)$ being close to being on-shell, it can produce some enhancement of the amplitudes, and (part of) the strong phases come from the absorptive part of the $f_0(1710)$ lineshape; see also Ref. [44]. We note that the imprints of resonances should manifest in the phase shifts and inelasticity that are the inputs of the DRs discussed previously.

The full contribution of isospin-zero-only amplitudes to the denominator of the CP asymmetries is lengthy. Keeping only the terms in $|\lambda_d|^2$, $|\lambda_s|^2$, and $\text{Re}\{Q_{udcs}\}$, i.e., neglecting $|\lambda_b|^2$, $\text{Re}\{Q_{udcb}\}$, and $\text{Re}\{Q_{uscb}\}$ (or, alternatively, neglecting contributions from penguin operators), we have

$$\begin{aligned}
\text{den}(A_{CP}^i)_{I=0} &= 2(|\lambda_d|^2|\Omega_{i1}^{(0)}|^2(T_{\pi\pi}^{CC})^2 + |\lambda_s|^2|\Omega_{i2}^{(0)}|^2(T_{KK}^{CC})^2 \\
&\quad + 2\text{Re}\{Q_{udcs}\}\omega_i^{(\text{Re})}T_{\pi\pi}^{CC}T_{KK}^{CC}) \\
&\approx 2|\lambda_d|^2(|\Omega_{i1}^{(0)}|^2(T_{\pi\pi}^{CC})^2 + |\Omega_{i2}^{(0)}|^2(T_{KK}^{CC})^2 \\
&\quad - 2\omega_i^{(\text{Re})}T_{\pi\pi}^{CC}T_{KK}^{CC}), \quad (38)
\end{aligned}$$

where $\omega_i^{(\text{Re})} \equiv \text{Re}\{\Omega_{i1}^{(0)*}\Omega_{i2}^{(0)}\}$; in what will follow, $\omega_1^{(\text{Re})} \equiv \omega_\pi^{(\text{Re})}$ and $\omega_2^{(\text{Re})} \equiv \omega_K^{(\text{Re})}$. Numerically,

$$J/|\lambda_d|^2 = r_{\text{CKM}} \simeq 6.2 \times 10^{-4}, \quad (39)$$

so the numerator is typically much smaller than the denominator.

The previous exercise can be easily extended to isospin-two ($\pi\pi$) and isospin-one (KK) contributions, which we assume to be elastic. Although these are single-channel amplitudes, they can also lead to contributions to the CP asymmetries when interfering with the corresponding isospin-zero contributions. Adopting the parametrization $\Omega^{(1,2)} = |\Omega^{(1,2)}|e^{i\phi_{1,2}}$ (these quantities will later be extracted from branching ratios), one derives similar expressions in terms of rephasing-invariant quantities. The combinations analogous to $\omega_i^{(\text{Im})}$ above are now

$$\frac{\tilde{\omega}_{\pi i}^{(\text{Im})}}{|\Omega^{(2)}|} \equiv \text{Im}\{\Omega_{i1}^{(0)}e^{-i\phi_2}\}, \quad (40)$$

$$\frac{\tilde{\omega}_K^{(\text{Im})}}{|\Omega^{(1)}|} \equiv \text{Im}\{\Omega_{21}^{(0)*}e^{i\phi_1}\}, \quad (41)$$

where ϕ_2 (ϕ_1) is the strong phase developed by the isospin-two (respectively, isospin-one) amplitude. Appearing in the branching ratios, we have the following extra quantities:

$$\frac{\tilde{\omega}_{\pi i}^{(\text{Re})}}{|\Omega^{(2)}|} \equiv \text{Re}\{\Omega_{i1}^{(0)}e^{-i\phi_2}\}, \quad (42)$$

$$\frac{\tilde{\omega}_{Ki}^{(\text{Re})}}{|\Omega^{(1)}|} \equiv \text{Re}\{\Omega_{2i}^{(0)*}e^{i\phi_1}\}. \quad (43)$$

B. Rescattering parameters

Following the previous discussion, we have the following 17 parameters describing rescattering effects:

$$\begin{aligned}
 & \omega_\pi^{(\text{Im})}, \omega_K^{(\text{Im})}, \tilde{\omega}_{\pi 1}^{(\text{Im})}, \tilde{\omega}_{\pi 2}^{(\text{Im})}, \tilde{\omega}_K^{(\text{Im})}, \\
 & \tilde{\omega}_{\pi 1}^{(\text{Re})}, \tilde{\omega}_{\pi 2}^{(\text{Re})}, \tilde{\omega}_{K 1}^{(\text{Re})}, \tilde{\omega}_{K 2}^{(\text{Re})}, \\
 & |\Omega_{11}^{(0)}|^2, |\Omega_{12}^{(0)}|^2, |\Omega_{21}^{(0)}|^2, |\Omega_{22}^{(0)}|^2, \\
 & \omega_\pi^{(\text{Re})}, \omega_K^{(\text{Re})}, |\Omega^{(1)}|, |\Omega^{(2)}|,
 \end{aligned} \tag{44}$$

which are functions of the 12 parameters $\text{Re}\{\Omega_{ij}^{(0)}\}$, $\text{Im}\{\Omega_{ij}^{(0)}\}$, $|\Omega^{(1,2)}|$, $\phi_{1,2}$, $i, j = 1, 2$. The parameters $|\Omega^{(1)}|$ and $|\Omega^{(2)}|$ can be directly extracted from the branching ratios $D^+ \rightarrow K_S K^+$ and $D^+ \rightarrow \pi^0 \pi^+$, respectively. This results in the following⁹:

$$|\Omega^{(1)}| = 0.79, \quad |\Omega^{(2)}| = 0.90. \tag{45}$$

There are further four branching ratios of D^0 decays that depend linearly on 10 parameters, namely, $|\Omega_{11}^{(0)}|^2$, $|\Omega_{12}^{(0)}|^2$, $|\Omega_{21}^{(0)}|^2$, $|\Omega_{22}^{(0)}|^2$, $\tilde{\omega}_{\pi 1}^{(\text{Re})}$, $\tilde{\omega}_{\pi 2}^{(\text{Re})}$, $\tilde{\omega}_{K 1}^{(\text{Re})}$, $\tilde{\omega}_{K 2}^{(\text{Re})}$, $\omega_\pi^{(\text{Re})}$, $\omega_K^{(\text{Re})}$ (that depend on the 10 quantities $\text{Re}\{\Omega_{ij}^{(0)}\}$, $\text{Im}\{\Omega_{ij}^{(0)}\}$, and $\phi_{1,2}$). Therefore, by using only the branching ratios, the set of these parameters remains under-constrained.

However, the numerators of the CP asymmetries only depend on the five remaining parameters, namely, $\omega_\pi^{(\text{Im})}$, $\omega_K^{(\text{Im})}$, $\tilde{\omega}_{\pi 1}^{(\text{Im})}$, $\tilde{\omega}_{\pi 2}^{(\text{Im})}$, $\tilde{\omega}_K^{(\text{Im})}$. Fixing the denominators of the CP asymmetries, which are proportional to the branching ratios, to their experimental values, we have then that the four CP asymmetries of the $D^0 \rightarrow \pi^- \pi^+$, $\pi^0 \pi^0$, $K^- K^+$, $K_S K_S$ modes depend linearly on five parameters. Using the measurements by LHCb [2,3] is not enough then to determine ranges for the remaining two CP asymmetries in the final modes containing neutral pions and kaons. In a companion paper [96], we discuss how the use of the determinant of the Omnès matrix, which has the great advantage of being independent of the inelasticity, helps in setting ranges for the rescattering parameters controlling the level of CP asymmetry. Moreover, as discussed therein, the use of Eq. (11) leads to an additional relation, namely,

$$\text{Im}\{\Omega^{(0)\dagger}(s)\Sigma\Omega^{(0)}(s)\} = 0 \Rightarrow \sigma_\pi \omega_\pi^{(\text{Im})} + \sigma_K \omega_K^{(\text{Im})} = 0 \tag{46}$$

which implies that $\omega_\pi^{(\text{Im})}$ and $\omega_K^{(\text{Im})}$ have opposite signs, and similar absolute values, thus reducing the number of parameters controlling the CP asymmetries to 4.

The dependence of the CP asymmetries on the rescattering parameters is illustrated in the previous to the last column of Table II. Note that the interference terms

⁹Hereafter, the Wilson coefficients and quark masses are taken at 2 GeV.

$I = 0/I = 2$, $I = 2/I = 2$, $I = 0/I = 1$, and $I = 1/I = 1$ are sources of difference among pion and kaon channels independently of the rescattering parameters. On the other hand, the interference terms $I = 0/I = 0$ for pions and kaons have the same prefactors, see Eqs. (36) and (38), and the difference comes from the rescattering parameters, namely, $|\omega_\pi^{(\text{Im})}| \neq |\omega_K^{(\text{Im})}|$, $|\Omega_{11}^{(0)}|^2 \neq |\Omega_{21}^{(0)}|^2$, $|\Omega_{12}^{(0)}|^2 \neq |\Omega_{22}^{(0)}|^2$, $|\omega_\pi^{(\text{Re})}| \neq |\omega_K^{(\text{Re})}|$.

In the following section, except for $|\Omega^{(1)}|$ and $|\Omega^{(2)}|$, for which we consider Eq. (45), the remaining rescattering parameters in Eq. (44) are extracted from the use of DRs.

C. Results based on DRs

Before discussing predictions for CP asymmetries, we need to ensure that branching ratios can be correctly reproduced. Rescattering effects in isospin zero are given in Table I for various situations.¹⁰ We find that Omnès solutions resulting from solutions II and III, and solutions B' and C' do not lead to branching ratios of charm-meson decays in agreement with their experimental values, simultaneously for all four $D^0 \rightarrow \pi^- \pi^+$, $\pi^0 \pi^0$, $K^- K^+$, and $K_S K_S$ transitions. However, we highlight that a set of solutions is found satisfying the latter constraint, resulting from solution I for the phase shift δ_0^0 and inelasticity, and given in the first column of Table I. As previously stated, the profile of the inelasticity carries a large uncertainty, and solutions leading to the correct branching ratios are found when varying the inelasticity inside its error bar towards smaller values (i.e., away from the elastic limit), referred to as $\eta_0^0 - \delta\eta_0^0$. We display in Table I three such solutions, that differ in the way the asymptotic value of the inelasticity is approached, corresponding to different values of m_η^* . In what follows, the reference case refers to $m_\eta^* = 2$, although $m_\eta^* = 1$ or $m_\eta^* = 3$ lead to similar Omnès solutions.

Having selected the Omnès solutions based on the branching ratios, we then predict the CP asymmetries. In Table II we give numerical details about the predictions of CP asymmetries in charm-meson decays. Observables are illustrated in Fig. 4. Two cases of the phase shift ϕ_2 for isospin two lead to the correct branching ratios simultaneously for $\pi^0 \pi^0$ and $\pi^- \pi^+$, namely, $\phi_2 \simeq \pm\pi$, and $\phi_2 \simeq 0$,

¹⁰For illustrative purposes only, the procedure of Refs. [28,102] leads to $(S_S^{1/2} = \pm O\sigma D^{1/2} O^T$ if $S_S = ODO^T$, where O is an orthogonal matrix, D is a diagonal matrix, and σ is another diagonal matrix with ± 1 elements):

$$\begin{aligned}
 S_S^{1/2}(M_D^2) &= \pm \begin{pmatrix} 0.68e^{-0.61i} & 0.74e^{+1.05i} \\ 0.74e^{+1.05i} & 0.68e^{-0.44i} \end{pmatrix}, \\
 \text{or } S_S^{1/2}(M_D^2) &= \pm \begin{pmatrix} 0.74e^{-2.02i} & 0.67e^{+2.62i} \\ 0.67e^{+2.62i} & 0.74e^{-2.17i} \end{pmatrix}
 \end{aligned} \tag{47}$$

when using the same inputs used to generate the reference solution.

TABLE II. Budget of contributions to the CP asymmetries. The column “final numerics” corresponds to the values found at Eq. (48). When two values are provided, the first corresponds to the charged channels ($D^0 \rightarrow \pi^- \pi^+$ and $D^0 \rightarrow K^- K^+$), while the second to the neutral ones ($D^0 \rightarrow \pi^0 \pi^0$ and $D^0 \rightarrow K_S K_S$). For the CP asymmetries of each channel, divide the sum of the corresponding “numerator” terms by the sum of the “denominator” ones.

$A_{CP}(\pi^- \pi^+); A_{CP}(\pi^0 \pi^0)$	Interference	Expression	Final numerics
Numerator	$I = 0/I = 0$	$0.0019 \times \omega_\pi^{(\text{Im})}$	0.00027
	$I = 0/I = 2$	$0.00041 \times \tilde{\omega}_{\pi 2}^{(\text{Im})} + 0.00026 \times \tilde{\omega}_{\pi 1}^{(\text{Im})};$ $-0.00081 \times \tilde{\omega}_{\pi 2}^{(\text{Im})} - 0.00052 \times \tilde{\omega}_{\pi 1}^{(\text{Im})}$	-0.00009; 0.00018
Denominator	$I = 0/I = 0$	$ \Omega_{11}^{(0)} ^2 + 0.57 \times \Omega_{12}^{(0)} ^2 - 1.51 \times \omega_\pi^{(\text{Re})}$	1.11
	$I = 0/I = 2$	$0.64 \times \tilde{\omega}_{\pi 1}^{(\text{Re})} - 0.49 \times \tilde{\omega}_{\pi 2}^{(\text{Re})};$ $-1.28 \times \tilde{\omega}_{\pi 1}^{(\text{Re})} + 0.97 \times \tilde{\omega}_{\pi 2}^{(\text{Re})}$	0.03; -0.07
	$I = 2/I = 2$	$ \Omega^{(2)} ^2 \times 0.10; \Omega^{(2)} ^2 \times 0.41$	0.08; 0.33
<hr/>			
$A_{CP}(K^- K^+); A_{CP}(K_S K_S)$	Interference	Expression	Final numerics
Numerator	$I = 0/I = 0$	$0.0019 \times \omega_K^{(\text{Im})}$	-0.00032
	$I = 0/I = 1$	$0.0019 \times \tilde{\omega}_K^{(\text{Im})};$ $-0.0019 \times \tilde{\omega}_K^{(\text{Im})}$	-0.00019; 0.00019
Denominator	$I = 0/I = 0$	$ \Omega_{21}^{(0)} ^2 + 0.57 \times \Omega_{22}^{(0)} ^2 - 1.51 \times \omega_K^{(\text{Re})}$	1.05
	$I = 0/I = 1$	$1.15 \times \tilde{\omega}_{K 2}^{(\text{Re})} - 1.51 \times \tilde{\omega}_{K 1}^{(\text{Re})};$ $-1.15 \times \tilde{\omega}_{K 2}^{(\text{Re})} + 1.51 \times \tilde{\omega}_{K 1}^{(\text{Re})}$	1.23; -1.23
	$I = 1/I = 1$	$ \Omega^{(1)} ^2 \times 0.57$	0.36

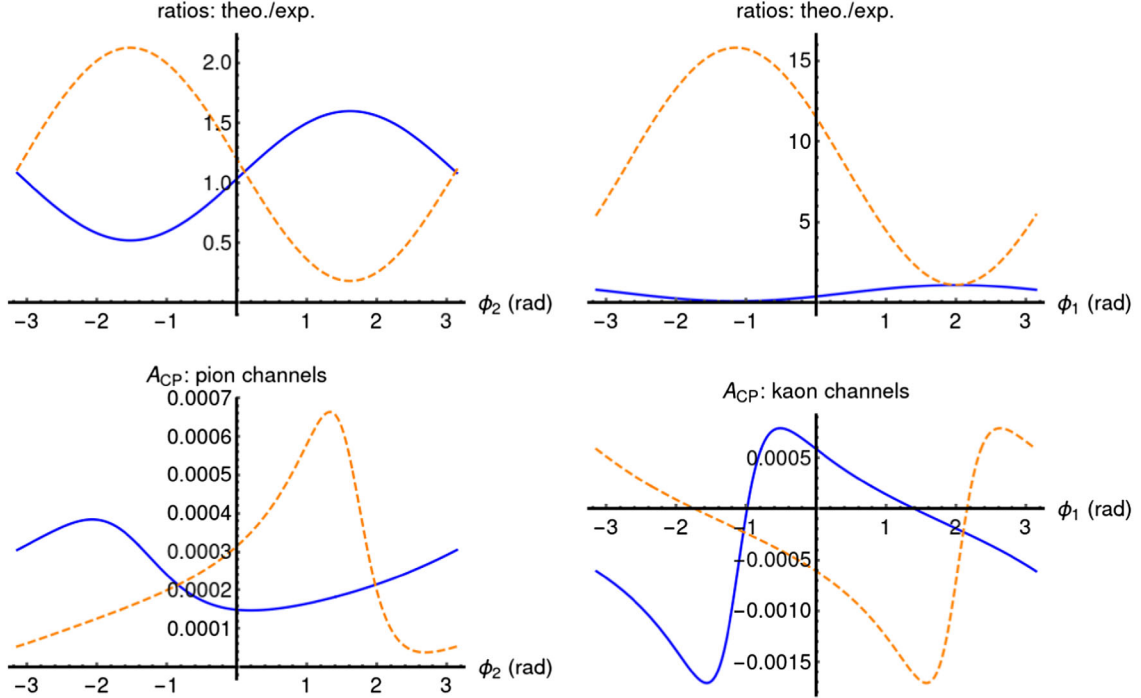


FIG. 4. Physical predictions for the reference case of Table I. Charged modes are shown in solid blue, while neutral ones are shown in dashed orange. Left (right) panels correspond to pion (kaon) modes. The top panels show the ratio of the theoretical and experimental $D^0 \rightarrow P^- P^+$ branching ratios, as function of the relevant ϕ_i phases, while the lower panels display the corresponding CP asymmetries.

which is closer to Ref. [86] and should therefore be preferred. In the reference case of Table I:

$$\begin{aligned}
 \omega_\pi^{(\text{Im})} &= 0.15, & \tilde{\omega}_{\pi 1}^{(\text{Im})} &= 0.53, & \tilde{\omega}_{\pi 2}^{(\text{Im})} &= -0.57, \\
 \omega_K^{(\text{Im})} &= -0.17, & \tilde{\omega}_K^{(\text{Im})} &= -0.1, \\
 |\Omega_{11}^{(0)}|^2 &= 0.34, & |\Omega_{12}^{(0)}|^2 &= 0.42, & \omega_\pi^{(\text{Re})} &= -0.35, \\
 |\Omega_{21}^{(0)}|^2 &= 0.35, & |\Omega_{22}^{(0)}|^2 &= 0.38, & \omega_K^{(\text{Re})} &= -0.32, \\
 \tilde{\omega}_{\pi 1}^{(\text{Re})} &= -0.07, & \tilde{\omega}_{\pi 2}^{(\text{Re})} &= -0.16, \\
 \tilde{\omega}_{K 1}^{(\text{Re})} &= -0.45, & \tilde{\omega}_{K 2}^{(\text{Re})} &= 0.47.
 \end{aligned} \tag{48}$$

These values correspond to $\phi_2 \simeq 0$, $\phi_1 = 2.0$. For $\phi_2 = \pm\pi$, $\tilde{\omega}_{\pi 1}^{(\text{Im})}$, $\tilde{\omega}_{\pi 2}^{(\text{Im})}$, $\tilde{\omega}_{\pi 1}^{(\text{Re})}$, $\tilde{\omega}_{\pi 2}^{(\text{Re})}$ flip signs with respect to $\phi_2 = 0$.

In both cases of ϕ_2 , the main contribution to the CP asymmetry $D^0 \rightarrow \pi^- \pi^+$ ($D^0 \rightarrow K^- K^+$) comes from the interference term $I = 0/I = 0$ (as well, $I = 0/I = 0$), followed closely by $I = 0/I = 2$ (respectively, $I = 0/I = 1$). For the $I = 0/I = 2$ contribution, we observe a cancellation due to the fact that $\tilde{\omega}_{\pi 1}^{(\text{Im})}$ and $\tilde{\omega}_{\pi 2}^{(\text{Im})}$ carry opposite signs. We obtain that the predicted values of the CP asymmetries are too small in the charged decay modes to reproduce the measured value of $\Delta A_{CP}^{\text{dir}}$ [2]. In the case of $\phi_2 \simeq 0$, the two interference terms, $I = 0/I = 2$ and $I = 0/I = 0$, contributing to $A_{CP}(D^0 \rightarrow \pi^- \pi^+)$ largely cancel, but they add up in the case $\phi_2 \simeq \pm\pi$. However, were there no cancellations (i.e., by artificially reversing signs to obtain a constructive pattern), the level of CP violation would remain small compared to the experimental measurement by LHCb. The value of the CP asymmetry for $D^0 \rightarrow K_S K_S$ is potentially large, at the price of a small branching ratio, see Appendix A.

As previously noticed, rescattering parameters are a source of breaking of a potential symmetry relating charm-meson decays into pion and kaon pairs: $|\omega_\pi^{(\text{Im})}| \neq |\omega_K^{(\text{Im})}|$ at the level of 20%, and $|\Omega_{12}^{(0)}|^2 \neq |\Omega_{22}^{(0)}|^2$ and $|\omega_\pi^{(\text{Re})}| \neq |\omega_K^{(\text{Re})}|$ at the level of 10%, while $|\Omega_{11}^{(0)}|^2 \simeq |\Omega_{21}^{(0)}|^2$. This breaking between isospin-zero amplitudes should be compared to the level of $SU(3)_F$ breaking found in decay constants and form factors, at the level of 20%; see Appendix A.

Further numerical information is provided in Table III. Note that rescattering effects lead to different strong phases for the isospin-zero amplitudes \mathcal{A}_0^π with respect to \mathcal{B}_0^π , and also \mathcal{A}_0^K with respect to \mathcal{B}_0^K . When $\Omega_{12}^{(0)} = 0$,

$$\tan(\arg \mathcal{A}_0^\pi) = \text{Im}[\Omega_{11}^{(0)}]/\text{Re}[\Omega_{11}^{(0)}] = \tan(\arg \mathcal{B}_0^\pi). \tag{49}$$

Also, when $\Omega_{21}^{(0)} = 0$,

TABLE III. Predictions based on the reference solution of Table I. The notation \mathcal{A} (\mathcal{B}) designates CP -even (respectively, CP -odd) amplitude components; ‘‘CV’’ stands for central value. When two numerical values are provided, the first corresponds to $\phi_2 \simeq 0$, while the second to $\phi_2 \simeq \pm\pi$.

$\mathcal{B}(D^0 \rightarrow \pi^- \pi^+)_{\text{theo,CV}}$	1.1
$\mathcal{B}(D^0 \rightarrow \pi^- \pi^+)_{\text{exp,CV}}$	
$\mathcal{B}(D^0 \rightarrow \pi^0 \pi^0)_{\text{theo,CV}}$	1.1
$\mathcal{B}(D^0 \rightarrow \pi^0 \pi^0)_{\text{exp,CV}}$	
$\mathcal{B}(D^+ \rightarrow \pi^0 \pi^+)_{\text{theo,CV}}$	Fixed to 1
$\mathcal{B}(D^+ \rightarrow \pi^0 \pi^+)_{\text{exp,CV}}$	
$A_{CP}(D^0 \rightarrow \pi^- \pi^+) \times 10^4$	2; 3
$A_{CP}(D^0 \rightarrow \pi^0 \pi^0) \times 10^4$	3; 0.5
$A_{CP}(D^+ \rightarrow \pi^0 \pi^+)$	0
$ \mathcal{A}_2^\pi \times 10^6$	$0.5 \times \Omega^{(2)} $
$ \mathcal{A}_0^\pi \times 10^6$	1.2
$ \mathcal{B}_2^\pi /r_{\text{CKM}} \times 10^6$	$0.5 \times \Omega^{(2)} $
$ \mathcal{B}_0^\pi /r_{\text{CKM}} \times 10^6$	0.8
$\arg(\mathcal{A}_0^\pi)$	93°
$\arg(\mathcal{B}_0^\pi)$	-72°
$\mathcal{B}(D^0 \rightarrow K^- K^+)_{\text{theo,CV}}$	1.1
$\mathcal{B}(D^0 \rightarrow K^- K^+)_{\text{exp,CV}}$	
$\mathcal{B}(D^0 \rightarrow K_S K_S)_{\text{theo,CV}}$	1.1
$\mathcal{B}(D^0 \rightarrow K_S K_S)_{\text{exp,CV}}$	
$\mathcal{B}(D^+ \rightarrow K_S K^+)_{\text{theo,CV}}$	Fixed to 1
$\mathcal{B}(D^+ \rightarrow K_S K^+)_{\text{exp,CV}}$	
$A_{CP}(D^0 \rightarrow K^- K^+) \times 10^4$	-2
$A_{CP}(D^0 \rightarrow K_S K_S) \times 10^4$	-7
$A_{CP}(D^+ \rightarrow K_S K^+)$	0
$ \mathcal{A}_{11}^K \times 10^6$	$0.8 \times \Omega^{(1)} $
$ \mathcal{A}_0^K \times 10^6$	1.1
$ \mathcal{B}_{11}^K /r_{\text{CKM}} \times 10^6$	$0.3 \times \Omega^{(1)} $
$ \mathcal{B}_0^K /r_{\text{CKM}} \times 10^6$	0.9
$\arg(\mathcal{A}_0^K)$	-66°
$\arg(\mathcal{B}_0^K)$	95°
$ \mathcal{A}_{13}^K , \mathcal{B}_{13}^K $	Sub-leading $\frac{1}{N_c}$

$$\tan(\arg \mathcal{A}_0^K) = \text{Im}[\Omega_{22}^{(0)}]/\text{Re}[\Omega_{22}^{(0)}] = \tan(\arg \mathcal{B}_0^K). \tag{50}$$

Having instead $\Omega_{12}^{(0)} \neq 0$ and/or $\Omega_{21}^{(0)} \neq 0$ allows then for contributions to the CP asymmetries coming from the interference term $I = 0/I = 0$.

The numerical conclusions made above do not depend significantly on the scale used for the Wilson coefficients and quark masses, which has been taken at 2 GeV in Eq. (45) and Tables II and III.

We stress that the work of a companion paper circumvents the need to discuss the input for the inelasticity [96], which carries a large uncertainty, and one achieves bounds on the CP asymmetries rather than predictions as above.

V. CONCLUSIONS

CP violation has been recently established in the charm sector, and its prediction based on the SM represents an

outstanding problem due to the presence of nonperturbative QCD effects. In charm physics, the mechanism of CP violation is expected to be largely influenced by such long-distance effects, while short-distance penguin contributions are expected to play a less important role. It is essential then to include rescattering effects in order to build an SM prediction of the recently measured CP asymmetries.

We have discussed a data-driven approach, which is based on the use of dispersion relations to take into account rescattering in the isospin-zero mode, with the subtraction constants being given by large N_C . Only pion and kaon pairs are included in the analysis, and further inelasticities are omitted. Given the large uncertainties attached to the pion-kaon inelasticity, we use $D^0 \rightarrow \pi^- \pi^+, \pi^0 \pi^0, K^- K^+, K_S K_S$ branching ratios to limit this source of hadronic uncertainties. We have also employed the charged decay modes $D^+ \rightarrow K_S K^+$ and $D^+ \rightarrow \pi^0 \pi^+$ to extract rescattering quantities for isospin one and two, respectively. There are four nonperturbative quantities controlling the CP asymmetries that are determined by the dispersion relations (a companion paper [96] discusses bounds on these quantities). Our main result is that CP asymmetries in the $D^0 \rightarrow \pi^- \pi^+$ and $D^0 \rightarrow K^- K^+$ decay modes are too small compared to the experimental value [2]. The main reason for this is not an accidental cancellation among contributions, but rather that rescattering effects turn out not producing enough enhancement. We also find that the level of $SU(3)_F$ breaking due to rescattering effects in isospin-zero amplitudes is similar to the one of decay constants and form factors.

In the future, we also plan to address further inelasticities. Their effect might be expected not to be too large though: in the cases of ρ pairs and $a_1(1260)\pi$, whose thresholds take place, respectively, at ~ 1.54 GeV and ~ 1.23 GeV, there is a phase-space suppression. Decay modes with $\eta^{(\prime)}$ are expected to give small contributions. In any case, if such effects are important this means that a similar level of CP violation already found experimentally

in $D^0 \rightarrow \pi^- \pi^+, K^- K^+$ should also be found in other charm-meson decay channels.

ACKNOWLEDGMENTS

We would like to thank especially Bachir Moussallam for many crucial discussions for the development of this project, in particular, concerning fundamental solutions of Ref. [7], the numeric method of Ref. [90], and off-diagonal T -matrix elements of Refs. [103,104]; also, Arkaitz Rodas for kindly providing further details and numerical files about Refs. [19,20]; finally, Miguel Albaladejo, Véronique Bernard, Joachim Brod, Sébastien Descotes-Genon, Hector Gisbert Mullor, Sebastian Jäger, Martin Jung, Patrícia C. Magalhães, Ulrich Nierste, Emilie Passemar, José R. Peláez, Marcos N. Rabelo, and Jaume Tarrús Castellà for useful discussions. This work has been supported by MCIN/AEI/10.13039/501100011033, Grants No. PID2020–114473 GB-I00 and No. PRE2018-085325, and by Generalitat Valenciana, Grant No. PROMETEO/2021/071. This project has received funding from the European Union’s Horizon 2020 research and innovation programme under the Marie Skłodowska-Curie Grant Agreement No. 101031558. L. V. S. is grateful for the hospitality of the CERN-TH group where part of this research was executed.

APPENDIX A: NUMERICAL INPUTS

The Wilson coefficients C_1, \dots, C_6 are given in Table IV, based in Ref. [62], at NLO in the naive dimensional regularization (NDR) scheme; one observes at this order a strong scheme dependence (NDR vs the ‘t Hooft-Veltman scheme), see Ref. [61].

The following values of the form factors and decay constants, obtained from lattice simulations with $N_f = 2 + 1 + 1$ active quark flavors, are taken from Ref. [105]; see also references therein:

TABLE IV. In the upper panel, the Wilson coefficients at NLO in the NDR scheme, with four dynamical flavors, see [62] and references therein; $\alpha_s(M_Z) = 0.1179$ (we employ its expression at NLO), $\mu_b = m_b$, with $m_b = 4.18$ GeV, and $M_W = 80.4$ GeV, $M_Z = 91.1876$ GeV, $m_t = 163.3$ GeV. The bottom panel gives the $\overline{\text{MS}}$ quark masses in MeV at $N_f = 2 + 1 + 1$, see [105] and references therein; the running factor 0.857 from m_c to 2 GeV has been employed.

μ	C_1	C_2	C_3	C_4	C_5	C_6
m_c	1.22	−0.40	0.021	−0.055	0.0088	−0.060
2 GeV	1.18	−0.32	0.011	−0.031	0.0068	−0.032
μ	m_u	m_d	$\hat{m} \equiv (m_u + m_d)/2$	m_s	m_c	
m_c	2.50 ± 0.09	5.48 ± 0.06	4.00 ± 0.06	109.0 ± 0.7	1280 ± 13	
2 GeV	2.14 ± 0.08	4.70 ± 0.05	3.427 ± 0.051	93.46 ± 0.58	1097 ± 11	

$$\begin{aligned}
 \frac{f_K}{f_\pi} &= 1.1934 \pm 0.0019, \\
 f_K &= (0.1557 \pm 0.0003) \text{ GeV}, \\
 f_D &= (0.2120 \pm 0.0007) \text{ GeV}, \\
 f_0^{D\pi}(0) &= 0.612 \pm 0.035, \\
 f_0^{DK}(0) &= 0.7385 \pm 0.0044. \tag{A1}
 \end{aligned}$$

We consider the following single-pole corrections to the form factors [51], which amount to a tiny correction

$$f_0^{D\pi}(M_\pi^2) = \frac{f_0^{D\pi}(0)}{1 - \frac{M_\pi^2}{M_{D_0^*}^2(2300)}}, \tag{A2}$$

$$f_0^{DK}(M_K^2) = \frac{f_0^{DK}(0)}{1 - \frac{M_K^2}{M_{D_{s0}^*}^2(2317)^\pm}}. \tag{A3}$$

For the meson masses we adopt the values: $M_\pi = 139.57$ MeV, $M_K = 496$ MeV, $M_D = 1864.84$ MeV, $M_{D_0^*}(2300) = (2343 \pm 10)$ MeV, $M_{D_{s0}^*}(2317)^\pm = (2317.8 \pm 0.5)$ MeV; $D^{0,\pm}$ lifetimes are $\tau_{D^\pm} = 1.033$ ps, and $\tau_{D^0} = 0.4103$ ps [93].

The entries of the CKM matrix are taken from the CKMfitter Spring '21 [106,107] values of the Wolfenstein parameters:

$$\begin{aligned}
 A &= 0.8132, & \lambda &= 0.22500, \\
 \bar{\rho} &= 0.1566, & \bar{\eta} &= 0.3475, \\
 \text{Re}\{\lambda_d\} &= -0.22, & \text{Im}\{\lambda_d\} &= 1.3 \times 10^{-4}, \\
 \text{Re}\{\lambda_s\} &= 0.22, & \text{Im}\{\lambda_s\} &= 6.9 \times 10^{-6}, \\
 \text{Re}\{\lambda_b\} &= 6.1 \times 10^{-5}, & \text{Im}\{\lambda_b\} &= -1.4 \times 10^{-4}. \tag{A4}
 \end{aligned}$$

The relevant branching ratios have the following numerical values [108]:

$$\begin{aligned}
 \mathcal{B}(K^-\pi^+) &= (3.999 \pm 0.006 \pm 0.031 \pm 0.032)\%, \\
 \mathcal{B}(\pi^-\pi^+) &= (0.1490 \pm 0.0012 \pm 0.0015 \pm 0.0019)\%, \\
 \mathcal{B}(K^-K^+) &= (0.4113 \pm 0.0017 \pm 0.0041 \pm 0.0025)\%, \tag{A5}
 \end{aligned}$$

with a correlation matrix

$$\begin{aligned}
 &\text{corr}(\mathcal{B}(K^-\pi^+), \mathcal{B}(\pi^-\pi^+), \mathcal{B}(K^-K^+)) \\
 &= \begin{pmatrix} 1.00 & 0.77 & 0.76 \\ 0.77 & 1.00 & 0.58 \\ 0.76 & 0.58 & 1.00 \end{pmatrix}, \tag{A6}
 \end{aligned}$$

and [93]

$$\begin{aligned}
 \mathcal{B}(D^0 \rightarrow \pi^0\pi^0) &= (0.826 \pm 0.025) \times 10^{-3}, \\
 \mathcal{B}(D^0 \rightarrow K_S K_S) &= (0.141 \pm 0.005) \times 10^{-3}, \\
 \mathcal{B}(D^+ \rightarrow \pi^0\pi^+) &= (1.247 \pm 0.033) \times 10^{-3}, \\
 \mathcal{B}(D^+ \rightarrow K_S K^+) &= (3.04 \pm 0.09) \times 10^{-3}, \\
 \mathcal{B}(D^+ \rightarrow K_L K^+) &= (3.21 \pm 0.11 \pm 0.11) \times 10^{-3}. \tag{A7}
 \end{aligned}$$

In addition to the recent measurements in Eqs. (1) and (3), experimental values have been determined for the following CP asymmetries (combining direct and indirect CP violation in the case of D^0 decays) [108]:

$$\begin{aligned}
 A_{CP}(D^0 \rightarrow \pi^0\pi^0) &= (-0.03 \pm 0.64)\%, \\
 A_{CP}(D^0 \rightarrow K_S K_S) &= (-1.9 \pm 1.0)\%, \\
 A_{CP}(D^+ \rightarrow K_S K^+) &= (-0.11 \pm 0.25)\%, \\
 A_{CP}(D^+ \rightarrow (K^0/\bar{K}^0)K^+) &= (+0.01 \pm 0.07)\%, \tag{A8}
 \end{aligned}$$

and [93]:

$$A_{CP}(D^+ \rightarrow K_L K^+) = (-4.2 \pm 3.2 \pm 1.2)\%. \tag{A9}$$

The inputs for phase shifts and inelasticity have been discussed in Sec. III A.

APPENDIX B: NUMERICAL SOLUTION OF THE DRs

1. Numerical method

We comment on the numerical method used to solve the DRs, which is based on the Legendre-Gauss quadrature [90,109] (an iteration strategy is followed by Refs. [64,99]). Consider the following homogeneous problem:

$$\begin{aligned}
 R(s) &= \frac{1}{\pi} \int_{4M^2}^{\infty} ds' \frac{1}{s' - s} X(s') R(s'), \\
 X(s') &= \tan \delta(s'), & R(s) &= \text{Re}(F(s)). \tag{B1}
 \end{aligned}$$

We start by writing two basic properties of Legendre functions [in the interval $-1 < z < 1$, $Q_j(z)$ is real; we take it real also outside this interval]¹¹:

$$\begin{aligned}
 \int_{-1}^1 du \frac{P_j(u)}{u - z} &= -2Q_j(z), \\
 \int_{-1}^1 du P_m(u) P_n(u) &= \delta_{mn} \frac{2}{2m + 1}. \tag{B2}
 \end{aligned}$$

We exploit this relation to write

¹¹There was an unexpected difficulty, seemingly undocumented, when using Python 3.0 built-in functions `lqn` and `lqmn`, which do not return correct values for $Q_j(u)$ for large negative u and/or for $u \gtrsim -1$.

$$\begin{aligned}
& \int_{-1}^1 du' \frac{1}{u' - u} Y(u') \\
& \approx - \sum_{j=0}^{N-1} (2j+1) Q_j(u) \int_{-1}^1 du' P_j(u') Y(u') \\
& \approx - \sum_{j=0}^{N-1} (2j+1) Q_j(u) \\
& \quad \times \left[\sum_{i=1}^M w_i P_j(u_i) Y(u_i) + R_M(P_j Y) \right], \quad (\text{B3})
\end{aligned}$$

where in the first to second lines we exploit the relation among Legendre polynomials of first and second degrees, and in the second to third lines we execute a Gaussian quadrature, where the expressions for remainders in Gauss's formulas of quadrature integration are found in Ref. [110] (Chap. 25.4):

$$\begin{aligned}
R_M(f) &= \frac{2^{(2M+1)} (M!)^4}{(2M+1) [(2M)!]^3} \left. \frac{d^{(2M)} f(x)}{dx^{(2M)}} \right|_{x=\xi} \\
& \quad (-1 < \xi < 1). \quad (\text{B4})
\end{aligned}$$

Therefore, if the remainder $R_M(f)$ is sufficiently small,

$$\begin{aligned}
& \int_a^b ds' \frac{1}{s' - s_k} X(s') R(s') \\
& \approx \sum_{i=1}^M \hat{W}_i \left[1 + \frac{2(s_k - b)}{b - a} \right] X(s_i) R(s_i), \\
s_i &= \frac{a + b + (b - a)u_i}{2}, \quad (\text{B5})
\end{aligned}$$

$$\begin{aligned}
& \int_a^\infty ds' \frac{1}{s' - s_k} X(s') R(s') \\
& \approx \sum_{i=1}^M \hat{W}_i \left[1 - \frac{2a}{s_k} \right] \frac{s_i}{s_k} X(s_i) R(s_i), \\
s_i &= \frac{2a}{1 - u_i}, \quad (\text{B6})
\end{aligned}$$

$$\begin{aligned}
\hat{W}_i[z] &= -w_i \sum_{j=0}^{N-1} (2j+1) P_j(u_i) Q_j(z), \\
w_i &= \frac{2}{1 - u_i^2} \left[\frac{dP_M}{du}(u_i) \right]^{-2}. \quad (\text{B7})
\end{aligned}$$

In our case, we have subtractions and the system is inhomogeneous. For $n > 0$ subtractions, choosing s_0 on the real axis below the cut $s \geq 4M^2$,

$$\begin{aligned}
R(s) &= \sum_{k=0}^{n-1} \frac{(s - s_0)^k}{k!} R^{(k)}(s_0) \\
& \quad + \frac{(s - s_0)^n}{\pi} \int_{4M^2}^\infty ds' \frac{1}{s' - s} X(s') \frac{R(s')}{(s' - s_0)^n}, \quad (\text{B8})
\end{aligned}$$

with $R^{(k)}$ the k th derivative, for which a similar discussion holds.

Reference [90] chooses $M = N$, which typically we take to be ≈ 30 – 40 . Note that the method above leads to more sampling points close to the endpoints of the integration intervals. In the elastic region, the values of δ for which X diverges are then used as endpoints. In the inelastic region, the function appearing in the denominator of \mathbf{R}^{-1} in Eq. (22) has zeros, and the intervals of the numerical integration are chosen accordingly. The typical total number of integration intervals is ≈ 20 .

2. Dealing with the polynomial ambiguity

According to Ref. [7], there are n so-called fundamental functions $\chi^{(i)}(s)$, $i = 1, \dots, n$, of lowest finite degree in the n -channel coupled analysis. These solutions cannot be written as a polynomial times another solution. Their combination with polynomial coefficients is also a solution. The most general solution (having finite degree at infinity) is then

$$\sum_{i=1}^n P_i(s) \chi^{(i)}(s), \quad (\text{B9})$$

where $P_i(s)$ are polynomials of s , and the dimension of $\chi^{(i)}$ is n . For instance, in the two-channel coupled analysis, $\chi^{(i)}$ are vectors of dimension two.

Following the discussions of Sec. III and Appendix B 1, we generate the fundamental solutions in the latter two-channel coupled case numerically, satisfying the following condition at the subtraction point $s_0 < 4M^2$:

$$\begin{aligned}
(\chi^{(1)}(s_0) \otimes \chi^{(2)}(s_0)) &= \Omega^{(0)}(s_0) \\
&= (\mathcal{N}^{(1)}(s_0) \otimes \mathcal{N}^{(2)}(s_0)). \quad (\text{B10})
\end{aligned}$$

The numerical solutions $\mathcal{N}^{(i)}(s)$ are polynomials of degree 1 times the fundamental solutions $\chi^{(i)}(s)$, as it turns out that we find numerical solutions going asymptotically to non-vanishing constants, and that the indices $x_1 = x_2 = -1$; see Sec. III B. To get rid of the unknown polynomials, we also require that another condition is satisfied at a different point s_1 (in practice, $s_1 < s_0$):

$$(\mathcal{N}^{(1)}(s_1) \otimes \mathcal{N}^{(2)}(s_1)) = \begin{pmatrix} a_1 & a_3 \\ a_2 & a_4 \end{pmatrix}. \quad (\text{B11})$$

The values of $a_{1,2,3,4}$, which are real, are then adjusted in order to build the matrix $(\chi^{(1)}(s) \otimes \chi^{(2)}(s))$ that satisfies the condition valid for the determinant, Eq. (26), for which an explicit analytical expression is known. This procedure then leads to the sought system of fundamental solutions $\chi^{(i)}$. They are given at M_D^2 for various sets of inputs in Table I. The system of fundamental solutions is shown for

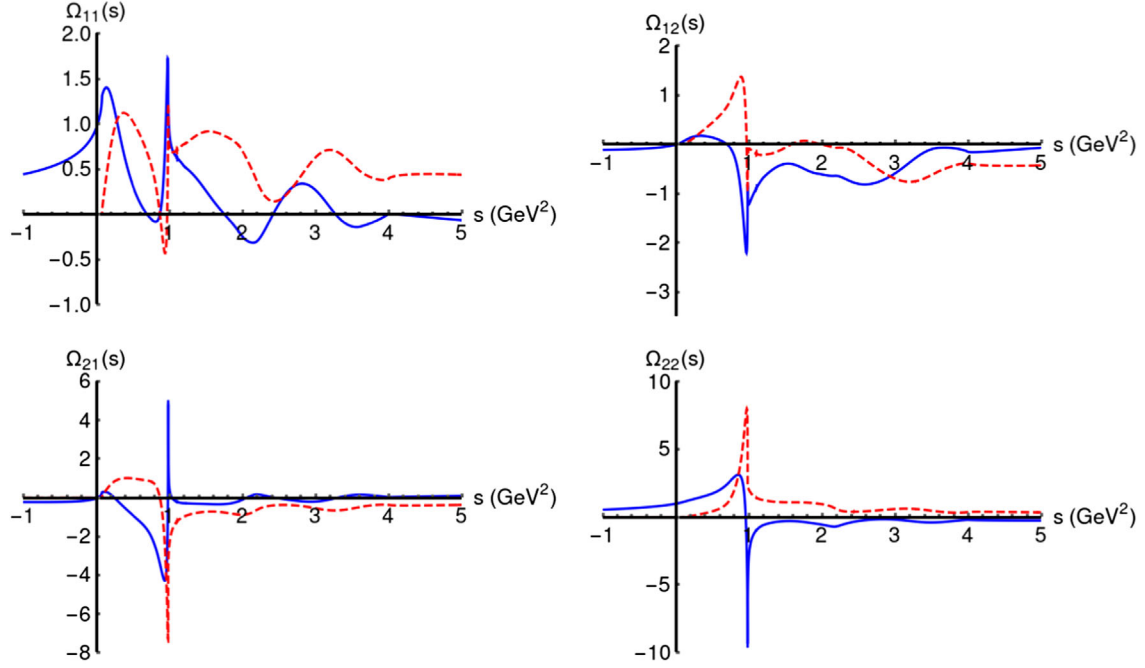


FIG. 5. Set of Omnès solutions for the reference case of Table I. Real parts are shown in solid blue, while imaginary parts are shown in dashed red.

the reference solution in Fig. 5. (As a cross-check, with the inputs used in Refs. [111,112], we have reproduced their Omnès solution.)

We reproduce from Ref. [7] the following properties of fundamental solutions that are used as checks of the previous algorithm:

PROPERTY 1^o: The determinant

$$\Delta(z) = \det \|\chi_\alpha^{(\beta)}(z)\| \quad (\alpha, \beta = 1, \dots, n) \quad (\text{B12})$$

does not vanish anywhere in the finite part of the plane.

PROPERTY 2^o: Let x_β be the degree of the solution $\chi^{(\beta)}(z)$ at infinity; if one defines

$$\chi^{(\beta),0}(z) = z^{-x_\beta} \chi^{(\beta)}(z) \quad (\beta = 1, 2, \dots, n), \quad (\text{B13})$$

then the determinant

$$\Delta^0(z) = \det \|\chi_\alpha^0(z)\| \quad (\text{B14})$$

has a finite nonzero value at infinity.

Crucially, by definition, any n solutions of the homogeneous Hilbert problem of Eq. (13) [where \mathcal{S} satisfies the Hölder condition ensuring it does not grow too fast with the energy [7], and its determinant does not vanish, see Eq. (26)], possessing properties 1^o and 2^o, is a fundamental system of solutions of this problem.

This latter step of getting rid of polynomial ambiguities has in practice been executed in *Mathematica* [113]. The numerical code implemented in Python together with a

Mathematica notebook containing an example will later be released in Zenodo.

APPENDIX C: EXPLICIT SOLUTION OF THE DRs CLOSE TO THE ELASTIC REGIME

It would be certainly important to achieve a full explicit analytical equation, instead of relying on a numerical method as described in the previous section, in order to get a higher understanding of the behavior of the Omnès solution given the required phase shifts and inelasticities as inputs. Hereafter, we discuss an explicit analytical expression for the amplitudes of the two-coupled channel problem valid close to the elastic limit. We write Eq. (11) as $A = S_S A^*$. This equation can be used to solve for the phases of the individual elements $A_{\pi\pi}, A_{KK}$ of $A \equiv (A_{\pi\pi}, A_{KK})^T$ as a function of the ratio of their magnitudes:

$$\begin{aligned} & \cos(\arg A_{\pi\pi}(s) - \delta_1(s)) \\ &= \sqrt{\frac{(1 + \eta(s))^2 - \lambda_{\pi K}^{-2}(s)(1 - \eta(s)^2)}{4\eta(s)}}, \end{aligned} \quad (\text{C1})$$

$$\begin{aligned} & \cos(\arg A_{KK}(s) - \delta_2(s)) \\ &= \sqrt{\frac{(1 + \eta(s))^2 - \lambda_{\pi K}^2(s)(1 - \eta(s)^2)}{4\eta(s)}}, \end{aligned} \quad (\text{C2})$$

where $\delta_1(s) = \delta_0^0(s)$, $\delta_2(s) = \psi_0^0(s) - \delta_0^0(s)$, $\eta(s) = \eta_0^0(s)$ in the isospin-zero case, and

$$\lambda_{\pi K}(s) \equiv \frac{|A_{\pi\pi}(s)|}{|A_{KK}(s)|}. \quad (\text{C3})$$

Exploiting the general once-subtracted relation arising from analyticity:

$$|A_i(s)| = |A_i(s_0)| \exp \left\{ \frac{s-s_0}{\pi} \int_{4M_K^2}^{\infty} dz \frac{\arg A_i(z)}{(z-s)(z-s_0)} \right\},$$

$$i = \pi\pi, KK, \quad (\text{C4})$$

where $A_i(s_0)$ collects the zeros of $A_i(s)$, and one obtains that the ratio of the magnitudes follows:

$$\begin{aligned} \lambda_{\pi K}(s) &= \lambda_{\pi K}(0) \\ &\times \exp \left\{ \frac{s}{\pi} \int_{4M_K^2}^{\infty} dz \frac{\delta_1(z) - \Theta(z-4M_K^2)\delta_2(z)}{z(z-s)} \right\} \\ &\times \exp \left\{ \frac{s}{\pi} \int_{4M_K^2}^{\infty} \frac{dz}{z(z-s)} \right. \\ &\times \left(\arccos \sqrt{\frac{(1+\eta(z))^2 - \lambda_{\pi K}^{-2}(z)(1-\eta(z)^2)}{4\eta(z)}} \right. \\ &\left. \left. - \arccos \sqrt{\frac{(1+\eta(z))^2 - \lambda_{\pi K}^2(z)(1-\eta(z)^2)}{4\eta(z)}} \right) \right\} \end{aligned} \quad (\text{C5})$$

for one subtraction taken at $s_0 = 0$.

Solving the latter equation is obviously a highly non-trivial task. However, close to the elastic limit $\eta(s) \sim 1$ for all relevant values of the energy s , we obtain the following approximation:

$$\lambda_{\pi K}^{-1}(s) - \lambda_{\pi K}(s) \simeq \phi_{el}(s) + \frac{s}{\pi} g_{el}(s) \int_{4M_K^2}^{\infty} dz \frac{\epsilon(z)\phi_{el}(z)}{z(z-s)} \quad (\text{C6})$$

after expansion in the small quantity $\epsilon(s)$

$$\epsilon(s) \equiv \sqrt{\frac{1-\eta(s)}{2}}. \quad (\text{C7})$$

The functions $\phi_{el}(s)$ and $g_{el}(s)$ are known from the perfect elastic limit $\eta(s) = 1$, they depend then only on the phase shifts $\delta_1(s)$, $\delta_2(s)$ and are given by

$$\phi_{el}(s) \equiv \lambda_{\pi K,el}^{-1}(s) - \lambda_{\pi K,el}(s), \quad (\text{C8})$$

$$g_{el}(s) \equiv -\lambda_{\pi K,el}^{-1}(s) - \lambda_{\pi K,el}(s), \quad (\text{C9})$$

where $\lambda_{\pi K,el}(s)$ the ratio of the amplitudes in the fully elastic case, given by the first two lines of Eq. (C5). Having

an approximation for the ratio $\lambda_{\pi K}(s)$, the phases of the individual amplitudes can be substituted in Eq. (C4) by the use of Eqs. (C1) and (C2), and $A_{\pi\pi}, A_{KK}$ can be obtained as functions of s . A drawback of this approach is that the ratio $\lambda_{\pi K,el}(s)$ may get close to zero, rendering ill defined the procedure described above, being well behaved for $\lambda_{\pi K,el}(s) \sim 1$. Because of these shortcomings, we stress that such a method, which illustrates the difficulty in obtaining an explicit analytical solution, has not been employed in the present work.

APPENDIX D: DECAY CONSTANTS AND FORM FACTORS

We need the following hadronic matrix elements of the axial vector (no sum over i, j is implied):

$$\langle 0 | \bar{q}^j \gamma^\mu \gamma_5 q^i | P^{ij}(p) \rangle = -\langle P^{ji}(p) | \bar{q}^j \gamma^\mu \gamma_5 q^i | 0 \rangle = i C_{P f_P}^{ij} p^\mu, \quad (\text{D1})$$

and vector,

$$\begin{aligned} \langle P'(p') | \bar{q}^j \gamma^\mu q^i | P(p) \rangle \\ = \tilde{C}_{P P'}^{ij} [(p+p')^\mu f_+^{P P'}(q^2) + (p-p')^\mu f_-^{P P'}(q^2)], \end{aligned} \quad (\text{D2})$$

QCD currents, where $q^\mu = p^\mu - p'^\mu$ and the superindices in $P^{ij} \sim q^i \bar{q}^j$ indicate the flavor content of the corresponding pseudoscalar meson (they are not displayed explicitly in the vector case where flavor quantum numbers can match in different ways).

In the axial-vector matrix element, the normalization of the decay constant corresponds to $f_\pi = \sqrt{2} F_\pi = (130.2 \pm 0.8)$ MeV [105]. The coefficient C_P^{ij} reflects the intrinsic flavor composition of P^{ij} . It is just equal to 1 for flavorful mesons, while for the flavorless states:

$$\begin{aligned} C_{\pi^0}^{11} &= -C_{\pi^0}^{22} = \frac{1}{\sqrt{2}}, \\ C_{\eta_8}^{11} &= C_{\eta_8}^{22} = -\frac{1}{2} C_{\eta_8}^{33} = \frac{1}{\sqrt{6}}, \\ C_{\eta_0}^{ii} &= \frac{1}{2}, \end{aligned} \quad (\text{D3})$$

$$C_{\eta_{15}}^{11} = C_{\eta_{15}}^{22} = C_{\eta_{15}}^{33} = -\frac{1}{3} C_{\eta_{15}}^{44} = \frac{1}{\sqrt{12}}. \quad (\text{D4})$$

These factors are conveniently captured in the following 4×4 matrix of pseudoscalar bosons [114]:

$$\Phi = \begin{pmatrix} \frac{\pi^0}{\sqrt{2}} + \frac{\eta_8}{\sqrt{6}} + \frac{\eta_{15}}{\sqrt{12}} + \frac{\eta_0}{2} & \pi^+ \\ \pi^- & -\frac{\pi^0}{\sqrt{2}} + \frac{\eta_8}{\sqrt{6}} + \frac{\eta_{15}}{\sqrt{12}} + \frac{\eta_0}{2} \\ K^- & \bar{K}^0 \\ D^+ & D^+ \\ & K^+ & \bar{D}^0 \\ & K^0 & D^- \\ -\frac{2\eta_8}{\sqrt{6}} + \frac{\eta_{15}}{\sqrt{12}} + \frac{\eta_0}{2} & D_s^- \\ & D_s^+ & -\frac{3\eta_{15}}{\sqrt{12}} + \frac{\eta_0}{2} \end{pmatrix}, \quad (\text{D5})$$

which fixes our conventions. Under charge conjugation $\Phi \rightarrow \Phi^T$. In the unphysical limit of vanishing quark masses, the axial quark current has the effective hadronic representation $\bar{q}^j \gamma^\mu \gamma_5 q^i \doteq -f \partial^\mu \Phi^{ij} + \mathcal{O}(\Phi^3)$, while the vector current is given by $\bar{q}^j \gamma_\mu q^i \doteq -i(\Phi \overleftrightarrow{\partial}_\mu \Phi)^{ij} + \mathcal{O}(\Phi^4)$ [11]. This reproduces the constant factors in Eq. (D4) and allows one to easily derive the appropriate Clebsch-Gordon coefficients in Eq. (D2), because the vector-current matrix element satisfies $f_+^{PP'}(0) = 1$ in the massless quark limit (vector-current conservation). We only quote here those coefficients needed in our calculation:

$$\begin{aligned} \tilde{C}_{D^+\pi^+}^{41} &= \sqrt{2} \tilde{C}_{D^0\pi^0}^{41} = \tilde{C}_{D^0\pi^-}^{42} \\ &= -\sqrt{2} \tilde{C}_{D^+\pi^0}^{42} = \tilde{C}_{D^0K^-}^{43} = \tilde{C}_{D^+\bar{K}^0}^{43} = 1. \end{aligned} \quad (\text{D6})$$

Since

$$q_\mu \langle P'(p') | \bar{q}^j \gamma^\mu q^i | P(p) \rangle = \tilde{C}_{PP'}^{ij} (M_P^2 - M_{P'}^2) f_0^{PP'}(q^2), \quad (\text{D7})$$

the scalar form factor

$$f_0^{PP'}(q^2) = f_+^{PP'}(q^2) + \frac{q^2}{M_P^2 - M_{P'}^2} f_-^{PP'}(q^2) \quad (\text{D8})$$

plays an important role in the bare decay amplitudes.

For the evaluation of the penguin contribution (Q_6), we also need the scalar and pseudoscalar matrix elements, which can be easily obtained by applying the QCD equations of motion:

$$\begin{aligned} \langle 0 | \bar{q}^j \gamma_5 q^i | P^{ij}(p) \rangle &= -i \frac{\langle 0 | \partial_\mu (\bar{q}^j \gamma^\mu \gamma_5 q^i) | P^{ij}(p) \rangle}{m_i + m_j} \\ &= -i C_P^{ij} \frac{f_P M_P^2}{m_i + m_j}, \end{aligned} \quad (\text{D9})$$

$$\begin{aligned} \langle P(p') | \bar{q}^j q^i | P(p) \rangle &= i \frac{\langle P(p') | \partial_\mu (\bar{q}^j \gamma^\mu q^i) | P(p) \rangle}{m_i - m_j} \\ &= \frac{\tilde{C}_P^{ij}}{m_i - m_j} (M_P^2 - M_{P'}^2) f_0^{PP'}(q^2). \end{aligned} \quad (\text{D10})$$

For equal quark masses the needed two-Goldstone matrix elements of the light-quark scalar currents,

$$\begin{aligned} \langle \pi^i | \bar{u}u + \bar{d}d | \pi^j \rangle &= \delta^{ij} F_S^\pi(t), \\ \langle K^+ | \bar{u}u | K^+ \rangle &= \langle K^+ | \bar{u}d | K^0 \rangle = \langle K^0 | \bar{d}d | K^0 \rangle = F_S^K(t), \end{aligned} \quad (\text{D11})$$

can be determined at low momentum transfer with χ PT [9,11]. At $\mathcal{O}(p^4)$ and keeping only the leading contributions at large- N_C , one gets

$$\begin{aligned} F_S^\pi(t) &= \frac{M_\pi^2}{\hat{m}} \left\{ 1 + \frac{16}{f_\pi^2} (2L_8 - L_5) M_\pi^2 + \frac{8L_5}{f_\pi^2} t \right\} \\ &\equiv \frac{M_\pi^2}{\hat{m}} \tilde{F}_S^\pi(t), \end{aligned} \quad (\text{D12})$$

$$\begin{aligned} F_S^K(t) &= \frac{M_K^2}{m_s + \hat{m}} \left\{ 1 + \frac{16}{f_K^2} (2L_8 - L_5) M_K^2 + \frac{8L_5}{f_K^2} t \right\} \\ &\equiv \frac{M_K^2}{m_s + \hat{m}} \tilde{F}_S^K(t), \end{aligned} \quad (\text{D13})$$

with $\hat{m} = m_u = m_d$. For the chiral low-energy constants we will adopt the values $L_5^r(M_\rho) = (1.20 \pm 0.10) \times 10^{-3}$ and $(2L_8^r - L_5^r)(M_\rho) = -(0.15 \pm 0.20) \times 10^{-3}$ [16].

APPENDIX E: BARE DECAY AMPLITUDES

The hadronic matrix elements of the four-quark operators in Eq. (8) are nonperturbative quantities, sensitive to the involved infrared properties of the strong interaction. However, they can be easily evaluated in the limit of a large number of QCD colors, because the product of two color-singlet quark currents factorizes at the hadron level into two current matrix elements [15,115]:

$$\langle J \cdot J \rangle = \langle J \rangle \langle J \rangle \left\{ 1 + \mathcal{O}\left(\frac{1}{N_C}\right) \right\}. \quad (\text{E1})$$

For instance, when $N_C \rightarrow \infty$,

$$\begin{aligned} \langle \pi^- \pi^+ | (\bar{d}c)_{V-A} (\bar{u}d)_{V-A} | D^0 \rangle &= \langle \pi^- | (\bar{d}c)_{V-A} | D^0 \rangle \langle \pi^+ | (\bar{u}d)_{V-A} | 0 \rangle \\ &= -\langle \pi^- | \bar{d} \gamma_\mu c | D^0 \rangle \langle \pi^+ | \bar{u} \gamma^\mu d | 0 \rangle \\ &= i f_\pi (M_D^2 - M_\pi^2) f_0^{D\pi}(M_\pi^2), \end{aligned} \quad (\text{E2})$$

while the penguin Q_6 operator gives

$$\begin{aligned}
& -2 \sum_q \langle \pi^- \pi^+ | (\bar{q}c)_{S-P} (\bar{u}q)_{S+P} | D^0 \rangle \\
& = 2 \langle 0 | \bar{u} \gamma_5 c | D^0 \rangle \langle \pi^- \pi^+ | \bar{u} u | 0 \rangle - 2 \langle \pi^- | \bar{d} c | D^0 \rangle \langle \pi^+ | \bar{u} \gamma_5 d | 0 \rangle \\
& = -2i \frac{M_\pi^2}{2\hat{m}} \left[\frac{f_D M_D^2}{m_c + \hat{m}} \tilde{F}_S^\pi(M_D^2) + \frac{f_\pi (M_D^2 - M_\pi^2)}{m_c - \hat{m}} f_0^{D\pi}(M_\pi^2) \right]. \tag{E3}
\end{aligned}$$

Using the matrix elements of the QCD currents given in Appendix D, one can then determine all bare decay amplitudes in the large- N_C limit:

$$\begin{aligned}
T_{D^0 \rightarrow \pi^- \pi^+}^{(B)} &= \frac{G_F}{\sqrt{2}} f_\pi (M_D^2 - M_\pi^2) f_0^{D\pi}(M_\pi^2) \\
&\quad \times [\lambda_d C_1 - \lambda_b (C_4 - C_6 \delta_6^\pi)], \\
T_{D^0 \rightarrow \pi^0 \pi^0}^{(B)} &= -\frac{G_F}{\sqrt{2}} f_\pi (M_D^2 - M_\pi^2) f_0^{D\pi}(M_\pi^2) \\
&\quad \times [\lambda_d C_2 + \lambda_b (C_4 - C_6 \delta_6^\pi)], \\
T_{D^+ \rightarrow \pi^0 \pi^+}^{(B)} &= -\frac{G_F}{\sqrt{2}} \frac{f_\pi}{\sqrt{2}} (M_D^2 - M_\pi^2) f_0^{D\pi}(M_\pi^2) \\
&\quad \times \lambda_d (C_1 + C_2), \\
T_{D^0 \rightarrow K^- K^+}^{(B)} &= \frac{G_F}{\sqrt{2}} f_K (M_D^2 - M_K^2) f_0^{DK}(M_K^2) \\
&\quad \times [\lambda_s C_1 - \lambda_b (C_4 - C_6 \delta_6^K)], \\
T_{D^0 \rightarrow \bar{K}^0 K^0}^{(B)} &= 0, \\
T_{D^+ \rightarrow \bar{K}^0 K^+}^{(B)} &= \frac{G_F}{\sqrt{2}} f_K (M_D^2 - M_K^2) f_0^{DK}(M_K^2) \\
&\quad \times [\lambda_s C_1 - \lambda_b (C_4 - C_6 \delta_6^K)], \tag{E4}
\end{aligned}$$

where

$$\delta_6^\pi = \frac{2}{m_c - \hat{m}} \frac{M_\pi^2}{2\hat{m}} \left\{ 1 + \frac{f_D M_D^2}{f_\pi (M_D^2 - M_\pi^2)} \frac{m_c - \hat{m}}{m_c + \hat{m}} \frac{\tilde{F}_S^\pi(M_D^2)}{f_0^{D\pi}(M_\pi^2)} \right\}, \tag{E5}$$

$$\begin{aligned}
\delta_6^K &= \frac{2}{m_c - m_s} \frac{M_K^2}{m_s + \hat{m}} \left\{ 1 \right. \\
&\quad \left. + \frac{f_D M_D^2}{f_K (M_D^2 - M_K^2)} \frac{m_c - m_s}{m_c + \hat{m}} \frac{\tilde{F}_S^K(M_D^2)}{f_0^{DK}(M_K^2)} \right\}. \tag{E6}
\end{aligned}$$

The conservation of the vector current guarantees that annihilation topologies give zero contribution, except for Q_6 which has a scalar-pseudoscalar structure. The matrix elements of Q_3 and Q_5 are also identically zero at $N_C \rightarrow \infty$ because $\sum_i \bar{q}_i \gamma_\mu \gamma_5 q_i$ only couples to isosinglet states.

The bare decay amplitudes involve the hadronic parameters f_π , f_K , $f_0^{D\pi}(M_\pi^2)$ and $f_0^{DK}(M_K^2)$, which we take from lattice calculations. These ‘‘physical’’ inputs include higher-order contributions in the $1/N_C$ expansion, dressing in this

way the current matrix elements beyond the large- N_C approximation. These additional corrections are totally independent of the rescattering dynamics incorporated in $\Omega^{(I)}(s)$.

A subtlety arises with the annihilation contribution to the matrix elements of the operator Q_6 , given for the $\pi^+ \pi^-$ case by the first term in Eq. (E3). This introduces the parameters $F_S^\pi(M_D^2)$ and $F_S^K(M_D^2)$ at $N_C \rightarrow \infty$, which are subjected to a large uncertainty. Their physical values at $N_C = 3$ are fully entangled with the rescattering dynamics of the final pair of pseudoscalars.¹² Using crossing symmetry, we input the χ PT predictions in Eq. (D12) at the subtraction point s_0 and let our calculated rescattering matrix generate the physical form factors at $s = M_D^2$.¹³

The global quark-mass factors in $\delta_6^{\pi,K}$ introduce an explicit dependence on the short-distance renormalization scale that exactly cancels the corresponding dependence of the Wilson coefficient $C_6(\mu^2)$ in the large- N_C limit. Q_6 is in fact the only four-quark operator with a nonzero anomalous dimension in the limit $N_C \rightarrow \infty$ [116]. In order to keep all short-distance logarithmic contributions, the Wilson coefficients are fully computed at NLO, without any $1/N_C$ expansion. Therefore, a subleading dependence on μ remains.

1. Isospin decomposition

Bose symmetry only allows an S -wave 2π state to have $I = 0$ and 2. In terms of isospin states $|I, I_3\rangle$ the 2π final states with definite charges are decomposed as¹⁴

$$|\pi^0 \pi^0\rangle = \sqrt{\frac{2}{3}} |2, 0\rangle - \frac{1}{\sqrt{3}} |0, 0\rangle,$$

$$\frac{1}{\sqrt{2}} |\pi^+ \pi^- + \pi^- \pi^+\rangle = -\frac{1}{\sqrt{3}} |2, 0\rangle - \sqrt{\frac{2}{3}} |0, 0\rangle,$$

$$\frac{1}{\sqrt{2}} |\pi^+ \pi^0 + \pi^0 \pi^+\rangle = -|2, 1\rangle. \tag{E7}$$

Therefore,¹⁵

¹²The calculation of these scalar form factors is interesting on its own. We defer to a forthcoming publication a detailed analysis of our predicted form factors and their comparison with previous calculations.

¹³Owing to the small value of $\text{Re}\{\lambda_b\}$, the D^0 decay branching ratios are not sensitive to the penguin operators and, therefore, the scalar form factors do not contaminate the specification of $\Omega^{(0)}(s)$.

¹⁴We adopt the usual isospin convention with quark multiplets (u, d) and $(-\bar{d}, \bar{u})$, and meson multiplets $(-\pi^+, \pi^0, \pi^-)$, (K^+, K^0) , $(-\bar{K}^0, K^-)$, (\bar{D}^0, D^-) , and $(-D^+, D^0)$, which is consistent with the matrix realization in Eq. (D5).

¹⁵ $\langle I^j I_3^j | O_{I_3} | I^i I_3^i \rangle = \langle I I_3 | I^j I_3^j | I I_3 \rangle \langle I^j | O_I | I^i \rangle$. The factor $1/\sqrt{2}$ in front of the $\pi^- \pi^+$ and $\pi^0 \pi^+$ amplitudes reabsorbs the phase-space factor for identical particles, so that one recovers the usual normalization of distinguishable particles adopted in the dynamical calculations.

$$\begin{aligned}
 A[D^0 \rightarrow \pi^0 \pi^0] &= -\frac{1}{\sqrt{6}} T_{\pi\pi}^0 + \frac{1}{\sqrt{3}} T_{\pi\pi}^2, \\
 A[D^0 \rightarrow \pi^- \pi^+] &\equiv \frac{1}{\sqrt{2}} A \left[D^0 \rightarrow \frac{1}{\sqrt{2}} (\pi^+ \pi^- + \pi^- \pi^+) \right] \\
 &= -\frac{1}{\sqrt{6}} T_{\pi\pi}^0 - \frac{1}{2\sqrt{3}} T_{\pi\pi}^2, \\
 A[D^+ \rightarrow \pi^0 \pi^+] &\equiv \frac{1}{\sqrt{2}} A \left[D^+ \rightarrow \frac{1}{\sqrt{2}} (\pi^+ \pi^0 + \pi^0 \pi^+) \right] \\
 &= \frac{\sqrt{3}}{2\sqrt{2}} T_{\pi\pi}^2. \tag{E8}
 \end{aligned}$$

The $K\bar{K}$ system can have $I = 0$ and $I = 1$:

$$\begin{aligned}
 |K^- K^+\rangle &= \frac{1}{\sqrt{2}} |1, 0\rangle - \frac{1}{\sqrt{2}} |0, 0\rangle, \\
 |\bar{K}^0 K^0\rangle &= -\frac{1}{\sqrt{2}} |1, 0\rangle - \frac{1}{\sqrt{2}} |0, 0\rangle, \\
 |\bar{K}^0 K^+\rangle &= -|1, 1\rangle. \tag{E9}
 \end{aligned}$$

This implies

$$\begin{aligned}
 A(D^0 \rightarrow K^- K^+) &= \frac{1}{2} (T_{KK}^{11} + T_{KK}^{13} - T_{KK}^0), \\
 A(D^0 \rightarrow \bar{K}^0 K^0) &= \frac{1}{2} (-T_{KK}^{11} - T_{KK}^{13} - T_{KK}^0), \\
 A(D^+ \rightarrow \bar{K}^0 K^+) &= T_{KK}^{11} - \frac{1}{2} T_{KK}^{13}. \tag{E10}
 \end{aligned}$$

Here, T_{KK}^{11} and T_{KK}^{13} denote the reduced amplitudes $\langle 1 || O_{1/2} || \frac{1}{2} \rangle$ and $\langle 1 || O_{3/2} || \frac{1}{2} \rangle$, respectively.

In the large- N_c limit, we get from Eq. (E4):

$$\begin{aligned}
 T_{\pi\pi}^{0(B)} &= -\frac{G_F}{\sqrt{2}} \sqrt{\frac{2}{3}} f_\pi (M_D^2 - M_\pi^2) f_0^{D\pi}(M_\pi^2) \\
 &\quad \times [\lambda_d(2C_1 - C_2) - 3\lambda_b(C_4 - C_6\delta_6^K)], \\
 T_{\pi\pi}^{2(B)} &= -\frac{G_F}{\sqrt{2}} \frac{2f_\pi}{\sqrt{3}} (M_D^2 - M_\pi^2) f_0^{D\pi}(M_\pi^2) \lambda_d(C_1 + C_2), \\
 -T_{KK}^{0(B)} &= T_{KK}^{11(B)} = \frac{G_F}{\sqrt{2}} f_K (M_D^2 - M_K^2) f_0^{DK}(M_K^2) \\
 &\quad \times [\lambda_s C_1 - \lambda_b(C_4 - C_6\delta_6^K)], \\
 T_{KK}^{13(B)} &= 0. \tag{E11}
 \end{aligned}$$

-
- [1] J. Charles *et al.*, Current status of the standard model CKM fit and constraints on $\Delta F = 2$ new physics, *Phys. Rev. D* **91**, 073007 (2015).
- [2] Roel Aaij *et al.*, Observation of CP Violation in Charm Decays, *Phys. Rev. Lett.* **122**, 211803 (2019).
- [3] Measurement of the time-integrated CP asymmetry in $D^0 \rightarrow K^- K^+$ decays, arXiv:2209.03179.
- [4] Elisabetta Pallante and Antonio Pich, Strong Enhancement of ϵ'/ϵ through Final State Interactions, *Phys. Rev. Lett.* **84**, 2568 (2000).
- [5] Elisabetta Pallante and Antonio Pich, Final state interactions in kaon decays, *Nucl. Phys.* **B592**, 294 (2001).
- [6] Kenneth M. Watson, Some general relations between the photoproduction and scattering of π mesons, *Phys. Rev.* **95**, 228 (1954).
- [7] N. I. Muskhelishvili, *Singular Integral Equations: Boundary Problems of Functions Theory and their Applications to Mathematical Physics* (Springer, New York, 1958).
- [8] R. Omnes, On the solution of certain singular integral equations of quantum field theory, *Nuovo Cimento* **8**, 316 (1958).
- [9] J. Gasser and H. Leutwyler, Chiral perturbation theory: Expansions in the mass of the strange quark, *Nucl. Phys.* **B250**, 465 (1985).
- [10] G. Ecker, Chiral perturbation theory, *Prog. Part. Nucl. Phys.* **35**, 1 (1995).
- [11] A. Pich, Chiral perturbation theory, *Rep. Prog. Phys.* **58**, 563 (1995).
- [12] E. Pallante, A. Pich, and I. Scimemi, The standard model prediction for ϵ'/ϵ , *Nucl. Phys.* **B617**, 441 (2001).
- [13] V. Cirigliano, A. Pich, G. Ecker, and H. Neufeld, Isospin Violation in ϵ' , *Phys. Rev. Lett.* **91**, 162001 (2003).
- [14] V. Cirigliano, G. Ecker, H. Neufeld, and A. Pich, Isospin breaking in $K \rightarrow \pi\pi$ decays, *Eur. Phys. J. C* **33**, 369 (2004).
- [15] Hector Gisbert and Antonio Pich, Direct CP violation in $K^0 \rightarrow \pi\pi$: Standard model status, *Rep. Prog. Phys.* **81**, 076201 (2018).
- [16] V. Cirigliano, H. Gisbert, A. Pich, and A. Rodríguez-Sánchez, Isospin-violating contributions to ϵ'/ϵ , *J. High Energy Phys.* **02** (2020) 032.
- [17] R. Kaminski, J. R. Pelaez, and F. J. Yndurain, The pion-pion scattering amplitude. III. Improving the analysis with forward dispersion relations and Roy equations, *Phys. Rev. D* **77**, 054015 (2008).
- [18] R. Garcia-Martin, R. Kaminski, J. R. Pelaez, J. Ruiz de Elvira, and F. J. Yndurain, The pion-pion scattering amplitude. IV: Improved analysis with once subtracted Roy-like equations up to 1100 MeV, *Phys. Rev. D* **83**, 074004 (2011).
- [19] J. R. Pelaez, A. Rodas, and J. Ruiz De Elvira, Global parameterization of $\pi\pi$ scattering up to 2 GeV, *Eur. Phys. J. C* **79**, 1008 (2019).

- [20] José R. Peláez and Arkaitz Rodas, Dispersive $\pi K \rightarrow \pi K$ and $\pi\pi \rightarrow K\bar{K}$ amplitudes from scattering data, threshold parameters and the lightest strange resonance κ or $K_0^*(700)$, *Phys. Rep.* **969**, 1 (2022).
- [21] Gerard 't Hooft, A planar diagram theory for strong interactions, *Nucl. Phys.* **B72**, 461 (1974).
- [22] Gerard 't Hooft, A two-dimensional model for mesons, *Nucl. Phys.* **B75**, 461 (1974).
- [23] Edward Witten, Baryons in the $1/n$ expansion, *Nucl. Phys.* **B160**, 57 (1979).
- [24] Aneesh V. Manohar, Large N QCD, in *Les Houches Summer School in Theoretical Physics, Session 68: Probing the Standard Model of Particle Interactions* (1998), Vol. 2, pp. 1091–1169.
- [25] A. Pich, Colorless mesons in a polychromatic world, in *The Phenomenology of Large N_c QCD* (2002), Vol. 5, pp. 239–258.
- [26] Luiz Vale Silva, Antonio Pich, and Eleftheria Solomonidi, Final-state interactions in the CP asymmetry of D meson two-body decays, *Proc. Sci. ICHEP2022* (2022) 748.
- [27] Eleftheria Solomonidi, Antonio Pich, and Luiz Vale Silva, CP violation in D decays to two pseudoscalars: An SM-based calculation, *Acta Phys. Pol. B Proc. Suppl.* **16**, 16 (2023).
- [28] Manfred Bauer, B. Stech, and M. Wirbel, Exclusive nonleptonic decays of D^- , D_s^- , and B -mesons, *Z. Phys. C* **34**, 103 (1987).
- [29] Enrico Franco, Satoshi Mishima, and Luca Silvestrini, The standard model confronts CP violation in $D^0 \rightarrow \pi^+\pi^-$ and $D^0 \rightarrow K^+K^-$, *J. High Energy Phys.* **05** (2012) 140.
- [30] Ignacio Bediaga, Tobias Frederico, and Patricia Magalhaes, Enhanced charm CP asymmetries from final state interactions, *Phys. Rev. Lett.* **131**, 051802 (2023).
- [31] Ulrich Nierste and Stefan Schacht, CP asymmetries in D decays to two pseudoscalars, *Proc. Sci. ICHEP2016* (2016) 527.
- [32] C. Sorensen, Final state interactions in the decays of charmed mesons, *Phys. Rev. D* **23**, 2618 (1981).
- [33] J.H. Reid and N.N. Trofimov, An application of unitarity to nonleptonic d decays, *Phys. Rev. D* **25**, 3078 (1982).
- [34] A. N. Kamal and R. Sinha, Coupled channel treatment of Cabibbo-angle-suppressed (D, D_s^+) $\rightarrow PP$ decays, *Phys. Rev. D* **36**, 3510 (1987).
- [35] A. N. Kamal, Two-body final state interactions with examples, *Int. J. Mod. Phys. A* **07**, 3515 (1992).
- [36] Andrzej Czarnecki, A. N. Kamal, and Qi-ping Xu, On $D \rightarrow \pi\pi$ and K anti- K decays, *Z. Phys. C* **54**, 411 (1992).
- [37] P. Zenczykowski, Nonleptonic charmed meson decays: Quark diagrams and final state interactions, *Acta Phys. Pol. B* **28**, 1605 (1997).
- [38] P. Zenczykowski, Coupled channel final state interactions through Reggeon exchange for $D(B) \rightarrow \pi\pi, K$ anti- K , *Phys. Lett. B* **460**, 390 (1999).
- [39] Joachim Brod, Alexander L. Kagan, and Jure Zupan, Size of direct CP violation in singly Cabibbo-suppressed D decays, *Phys. Rev. D* **86**, 014023 (2012).
- [40] Yuval Grossman and Dean J. Robinson, SU(3) sum rules for charm decay, *J. High Energy Phys.* **04** (2013) 067.
- [41] Gudrun Hiller, Martin Jung, and Stefan Schacht, SU(3)-flavor anatomy of nonleptonic charm decays, *Phys. Rev. D* **87**, 014024 (2013).
- [42] Stefan Schacht, A U-spin anomaly in charm CP violation, *J. High Energy Phys.* **03** (2023) 205.
- [43] Amarjit Soni, Resonance enhancement of charm CP , [arXiv:1905.00907](https://arxiv.org/abs/1905.00907).
- [44] Stefan Schacht and Amarjit Soni, Enhancement of charm CP violation due to nearby resonances, *Phys. Lett. B* **825**, 136855 (2022).
- [45] Franco Buccella, Ayan Paul, and Pietro Santorelli, SU(3) $_F$ breaking through final state interactions and CP asymmetries in $D \rightarrow PP$ decays, *Phys. Rev. D* **99**, 113001 (2019).
- [46] Hsiang-Nan Li, Cai-Dian Lü, and Fu-Sheng Yu, Implications on the first observation of charm CPV at LHCb, [arXiv:1903.10638](https://arxiv.org/abs/1903.10638).
- [47] H.-Y. Cheng and C.-W. Chiang, Direct CP violation in two-body hadronic charmed meson decays, *Phys. Rev. D* **85**, 034036 (2012).
- [48] H.-Y. Cheng and C.-W. Chiang, SU(3) symmetry breaking and CP violation in $D \rightarrow PP$ decays, *Phys. Rev. D* **86**, 014014 (2012).
- [49] Hai-Yang Cheng and Cheng-Wei Chiang, Revisiting CP violation in $D \rightarrow PP$ and VP decays, *Phys. Rev. D* **100**, 093002 (2019).
- [50] H.-Y. Cheng and C.-W. Chiang, CP violation in quasi-two-body $D \rightarrow VP$ decays and three-body D decays mediated by vector resonances, *Phys. Rev. D* **104**, 073003 (2021).
- [51] Sarah Müller, Ulrich Nierste, and Stefan Schacht, Topological amplitudes in D decays to two pseudoscalars: A global analysis with linear SU(3) $_F$ breaking, *Phys. Rev. D* **92**, 014004 (2015).
- [52] Sarah Müller, Ulrich Nierste, and Stefan Schacht, Sum Rules of Charm CP Asymmetries Beyond the SU(3) $_F$ Limit, *Phys. Rev. Lett.* **115**, 251802 (2015).
- [53] Ulrich Nierste and Stefan Schacht, CP violation in $D^0 \rightarrow K_S K_S$, *Phys. Rev. D* **92**, 054036 (2015).
- [54] Di Wang, Evidence of $A_{CP}(D^0 \rightarrow \pi^+\pi^-)$ implies observable CP violation in the $D^0 \rightarrow \pi^0\pi^0$ decay, *Eur. Phys. J. C* **83**, 279 (2023).
- [55] Alexander Khodjamirian and Alexey A. Petrov, Direct CP asymmetry in $D \rightarrow \pi^-\pi^+$ and $D \rightarrow K^-K^+$ in QCD-based approach, *Phys. Lett. B* **774**, 235 (2017).
- [56] Mikael Chala, Alexander Lenz, Aleksey V. Rusov, and Jakub Scholtz, ΔA_{CP} within the standard model and beyond, *J. High Energy Phys.* **07** (2019) 161.
- [57] Maxwell T. Hansen and Stephen R. Sharpe, Multiple-channel generalization of Lellouch-Lüscher formula, *Phys. Rev. D* **86**, 016007 (2012).
- [58] Yuval Grossman, Alexander L. Kagan, and Jure Zupan, Testing for new physics in singly Cabibbo suppressed D decays, *Phys. Rev. D* **85**, 114036 (2012).
- [59] Avital Dery and Yosef Nir, Implications of the LHCb discovery of CP violation in charm decays, *J. High Energy Phys.* **12** (2019) 104.
- [60] Rigo Bause, Hector Gisbert, Gudrun Hiller, Tim Höhne, Daniel F. Litim, and Tom Steudtner, Two is better than one: The U-spin- CP anomaly in charm, *Phys. Rev. D* **108**, 035005 (2023).

- [61] Gerhard Buchalla, Andrzej J. Buras, and Markus E. Lautenbacher, Weak decays beyond leading logarithms, *Rev. Mod. Phys.* **68**, 1125 (1996).
- [62] Stefan de Boer, Bastian Müller, and Dirk Seidel, Higher-order Wilson coefficients for $c \rightarrow u$ transitions in the standard model, *J. High Energy Phys.* **08** (2016) 091.
- [63] José Antonio Oller, *A Brief Introduction to Dispersion Relations*, SpringerBriefs in Physics (Springer, New York, 2019).
- [64] John F. Donoghue, J. Gasser, and H. Leutwyler, The decay of a light Higgs boson, *Nucl. Phys.* **B343**, 341 (1990).
- [65] G. Peter Lepage and Stanley J. Brodsky, Exclusive processes in perturbative quantum chromodynamics, *Phys. Rev. D* **22**, 2157 (1980).
- [66] O. Babelon, J.L. Basdevant, D. Caillerie, and G. Mennessier, Unitarity and inelastic final state interactions, *Nucl. Phys.* **B113**, 445 (1976).
- [67] Jose Ramon Pelaez, Arkaitz Rodas, and Jacobo Ruiz de Elvira, $f_0(1370)$ Controversy from Dispersive Meson-Meson Scattering Data Analyses, *Phys. Rev. Lett.* **130**, 051902 (2023).
- [68] R. Kaminski, L. Lesniak, and K. Rybicki, Separation of S wave pseudoscalar and pseudovector amplitudes in $\pi^- p$ (polarized) $\rightarrow \pi^+ \pi^- n$ reaction on polarized target, *Z. Phys. C* **74**, 79 (1997).
- [69] H. Becker *et al.*, A model independent partial wave analysis of the $\pi^+ \pi^-$ system produced at low four momentum transfer in the reaction $\pi^- p$ (polarized) $\rightarrow \pi^+ \pi^- n$ at 17.2-GeV/c, *Nucl. Phys.* **B151**, 46 (1979).
- [70] B. Hyams *et al.*, $\pi\pi$ phase shift analysis from 600-MeV to 1900-MeV, *Nucl. Phys.* **B64**, 134 (1973).
- [71] G. Grayer *et al.*, High statistics study of the reaction $\pi^- p \rightarrow \pi^- \pi^+ n$: Apparatus, method of analysis, and general features of results at 17-GeV/c, *Nucl. Phys.* **B75**, 189 (1974).
- [72] B. Hyams *et al.*, A study of all the $\pi\pi$ phase shift solutions in the mass region 1.0-GeV to 1.8-GeV from $\pi^- p \rightarrow \pi^- \pi^+ n$ at 17.2-GeV, *Nucl. Phys.* **B100**, 205 (1975).
- [73] Wolfgang Ochs, The status of glueballs, *J. Phys. G* **40**, 043001 (2013).
- [74] J.R. Pelaez and A. Rodas, $\pi\pi \rightarrow K\bar{K}$ scattering up to 1.47 GeV with hyperbolic dispersion relations, *Eur. Phys. J. C* **78**, 897 (2018).
- [75] Eugene P. Wigner, Lower limit for the energy derivative of the scattering phase shift, *Phys. Rev.* **98**, 145 (1955).
- [76] Roger G. Newton, *Scattering Theory of Waves and Particles*, Theoretical and Mathematical Physics (Springer, Berlin, Heidelberg, 1982).
- [77] Steven Weinberg, *Lectures on Quantum Mechanics* (Cambridge University Press, Cambridge, England, 2015), 2nd ed.
- [78] Arkaitz Rodas (private communication).
- [79] R. S. Longacre *et al.*, A measurement of $\pi^- p \rightarrow K^0(s) K^0(s) n$ at 22-GeV/c and a systematic study of the 2^{++} meson spectrum, *Phys. Lett. B* **177**, 223 (1986).
- [80] Daniel H. Cohen, D. S. Ayres, R. Diebold, S. L. Kramer, A. J. Pawlicki, and A. B. Wicklund, Amplitude analysis of the $K^- K^+$ system produced in the reactions $\pi^- p \rightarrow K^- K^+ n$ and $\pi^+ n \rightarrow K^- K^+ p$ at 6-GeV/c, *Phys. Rev. D* **22**, 2595 (1980).
- [81] A. Etkin *et al.*, Amplitude analysis of the $K_S^0 K_S^0$ system produced in the reaction $\pi^- p \rightarrow K_S^0 K_S^0 n$ at 23-GeV/c, *Phys. Rev. D* **25**, 1786 (1982).
- [82] Daniel H. Cohen, T. Ferbel, P. Slattery, and B. Werner, Study of $\pi\pi$ scattering in the isotopic spin-2 channel, *Phys. Rev. D* **7**, 661 (1973).
- [83] M. J. Losty, V. Chaloupka, A. Ferrando, L. Montanet, E. Paul, D. Yaffe, A. Zieminski, J. Alitti, B. Gandois, and J. Louie, A study of $\pi^- \pi^-$ scattering from $\pi^- p$ interactions at 3.93-GeV/c, *Nucl. Phys.* **B69**, 185 (1974).
- [84] W. Hoogland *et al.*, Measurement and analysis of the $\pi^+ \pi^+$ system produced at small momentum transfer in the reaction $\pi^6 + p \rightarrow \pi^+ \pi^+ n$ at 12.5-GeV, *Nucl. Phys.* **B126**, 109 (1977).
- [85] José R. Peláez (private communication).
- [86] N. B. Durusoy, M. Baubillier, R. George, M. Goldberg, A. M. Touchard, N. Armenise, M. T. Fogli Muciaccia, and A. Silvestri, Study of the $i = 2\pi\pi$ scattering from the reaction $\pi^- d \rightarrow \pi^- \pi^- p_s p$ at 9.0 gev/c, *Phys. Lett.* **45B**, 517 (1973).
- [87] B. S. Zou, F. Q. Wu, L. Li, and D. V. Bugg, Understanding $I = 2\pi\pi$ interaction, *AIP Conf. Proc.* **717**, 347 (2004).
- [88] I. Caprini, G. Colangelo, and H. Leutwyler, Regge analysis of the $\pi\pi$ scattering amplitude, *Eur. Phys. J. C* **72**, 1860 (2012).
- [89] Antonio Pich, Eleftheria Solomonidi, and Luiz Vale Silva (to be published).
- [90] Bachir Moussallam, N_f dependence of the quark condensate from a chiral sum rule, *Eur. Phys. J. C* **14**, 111 (2000).
- [91] H. Leutwyler, Electromagnetic form-factor of the pion, in *Continuous Advances in QCD 2002/ARKADYFEST (Honoring the 60th Birthday of Prof. Arkady Vainshtein)* (2002), Vol. 12, pp. 23–40.
- [92] R. L. Warnock, Existence of the many-channel N/D representation, *Il Nuovo Cimento A (1965–1970)* **50**, 894 (1967).
- [93] R. L. Workman *et al.*, Review of particle physics, *Prog. Theor. Exp. Phys.* **2022**, 083C01 (2022).
- [94] Igor Danilkin, Oleksandra Deineka, and Marc Vanderhaeghen, Data-driven dispersive analysis of the $\pi\pi$ and πK scattering, *Phys. Rev. D* **103**, 114023 (2021).
- [95] Oleksandra Deineka, Igor Danilkin, and Marc Vanderhaeghen, Dispersive analysis of the $\pi\pi$ and πK scattering data, in *10th International workshop on Chiral Dynamics* (2022), p. 3, [arXiv:2203.02215](https://arxiv.org/abs/2203.02215).
- [96] Antonio Pich, Eleftheria Solomonidi, and Luiz Vale Silva, Constraining the level of direct CP violation in charm-meson two-body decays.
- [97] Francisco Guerrero and Antonio Pich, Effective field theory description of the pion form-factor, *Phys. Lett. B* **412**, 382 (1997).
- [98] A. Pich and J. Portoles, The vector form-factor of the pion from unitarity and analyticity: A model independent approach, *Phys. Rev. D* **63**, 093005 (2001).
- [99] Alejandro Celis, Vincenzo Cirigliano, and Emilie Passemar, Lepton flavor violation in the Higgs sector and the role of hadronic τ -lepton decays, *Phys. Rev. D* **89**, 013008 (2014).
- [100] Gustavo C. Branco, Luis Lavoura, and Joao P. Silva, *CP Violation* (Clarendon Press, Oxford, 1999), Vol. 103.

- [101] Joachim Brod, Yuval Grossman, Alexander L. Kagan, and Jure Zupan, A consistent picture for large penguins in $D \rightarrow \pi^+\pi^-, K^+K^-$, *J. High Energy Phys.* **10** (2012) 161.
- [102] Christopher Smith, $SU(N)$ elastic rescattering in B and D decays, *Eur. Phys. J. C* **10**, 639 (1999).
- [103] Paul Buettiker, S. Descotes-Genon, and B. Moussallam, A new analysis of πK scattering from Roy and Steiner type equations, *Eur. Phys. J. C* **33**, 409 (2004).
- [104] R. Garcia-Martin and B. Moussallam, MO analysis of the high statistics Belle results on $\gamma\gamma \rightarrow \pi^+\pi^-, \pi^0\pi^0$ with chiral constraints, *Eur. Phys. J. C* **70**, 155 (2010).
- [105] Y. Aoki *et al.*, FLAG review 2021, *Eur. Phys. J. C* **82**, 869 (2022).
- [106] J. Charles, Andreas Hocker, H. Lacker, S. Laplace, F. R. Le Diberder, J. Malcles, J. Ocariz, M. Pivk, and L. Roos, CP violation and the CKM matrix: Assessing the impact of the asymmetric B factories, *Eur. Phys. J. C* **41**, 1 (2005).
- [107] J. Charles *et al.* (CKMfitter Group), Updated results and plots, available at: ckmfitter.in2p3.fr.
- [108] Yasmine Sara Amhis *et al.*, Averages of b -hadron, c -hadron, and τ -lepton properties as of 2021, *Phys. Rev. D* **107**, 052008 (2023).
- [109] Matthias Jamin, Jose Antonio Oller, and Antonio Pich, Strangeness changing scalar form-factors, *Nucl. Phys.* **B622**, 279 (2002).
- [110] M. Abramowitz and I. A. Stegun, *Handbook of Mathematical Functions: With Formulas, Graphs, and Mathematical Tables*, National Bureau of Standards Applied Mathematics Series Vol. 55 (Dover Publications Inc., 1972).
- [111] Jaume Tarrús Castellà and Emilie Passemar, Exotic to standard bottomonium transitions, *Phys. Rev. D* **104**, 034019 (2021).
- [112] Jaume Tarrús Castellà (private communication).
- [113] Wolfram Research, Inc., *Mathematica*, Version 12.0, Champaign, IL, 2019.
- [114] F. J. Botella, S. Noguera, and J. Portoles, Parameter—free calculation of $D \rightarrow PP$ in a weak gauged $U(4)_L \otimes U(4)_R$ chiral Lagrangian model, *Phys. Lett. B* **312**, 191 (1993).
- [115] A. J. Buras, J. M. Gerard, and R. Ruckl, $1/N$ expansion for exclusive and inclusive charm decays, *Nucl. Phys.* **B268**, 16 (1986).
- [116] William A. Bardeen, A. J. Buras, and J. M. Gerard, The $K \rightarrow \pi\pi$ decays in the large N limit: Quark evolution, *Nucl. Phys.* **B293**, 787 (1987).